Development and Implementation of a Mouldable Soft Magnetic Composite

Siesing, Leif

2016

Document Version:
Publisher's PDF, also known as Version of record

Link to publication

Citation for published version (APA):
Siesing, L. (2016). *Development and Implementation of a Mouldable Soft Magnetic Composite*. [Doctoral Thesis (compilation), Faculty of Engineering, LTH]. Department of Mechanical Engineering, Lund University.

Total number of authors:
1

Development and Implementation of a Mouldable Soft Magnetic Composite

Development and Implementation of a Mouldable Soft Magnetic Composite

Leif Siesing

DOCTORAL DISSERTATION
By due permission of the Faculty of Engineering, Lund University, Sweden. To be defended in Lecture Hall M:B, Maskinhuset, Lund University on Friday November 11th at 10:00.

Faculty opponent

Professor Svein Thore Hagen
Høgskolen i Telemark, Norway

DOKUMENTDATABLAD enl SIS 61 41 21

Organization
LUND UNIVERSITY
Department of Mechanical Engineering
Box 118
SE–221 00 LUND
Sweden

Author(s)
Leif Siesing

Document name
DOCTORAL DISSERTATION

Date of disputation
2016-11-11

Sponsoring organization

Title and subtitle
Development and Implementation of a Mouldable Soft Magnetic Composite

Abstract

Electrical machines, chokes and induction heaters are found in most homes, offices and factories all over the world. They are used to create movement, filtrate the power or to generate heat. A typical unit consist of a coil and a flux conductor material. Some of the materials have been established for over 100 years, while others are only a couple of decades old.

A new flux conductor material has been developed at the Division of Production and Materials Engineering at Lund University. The material is called soft magnetic mouldable composite (SM^2C). This thesis is focused on investigating the potential of this material and lay a knowledge foundation, wherein the material properties and manufacturing process of the material is tested and further developed, as well as the material composition. In order to use the full potential of the material a holistic view of all the materials involved is necessary. Both coil and insulation suitable for the mouldable soft magnetic composite are therefore studied. Tests are performed both on the separate materials, but also together in applications. Several motors and induction heaters were built and tested in different projects.

Results from the work show that by changing from solid copper tubes to litz wire and by using a flux conductor an increase of efficiency from 50–80 % to 98 % is possible. This is due to lower losses in the current conductor and higher flux linkage.

The possibility to mould the soft magnetic composite has interesting potential. It is shown that sensors, current conductors and other soft magnetic materials can be integrated directly into the composite. Also, the technology will provide a good thermal contact between the materials. This is especially important for the current conductor, which is usually the main heat source. A good contact will help conduct away the heat if the device is designed properly.

Other opportunities are opened with the new technology as well. The size of a moulded part has no limit, unlike for other soft magnetic composites that are usually pressed. It is possible to mould parts into almost any geometry, but it is also easy to machine the material if wanted.

Key words
Soft magnetic composite, Mouldable, Manufacturing, Powder, Thermal conductivity, Permeability, Magnetic loss, finite element analysis.

Classification system and/or index terms (if any)

Supplementary bibliographical information

Language
English

ISSN and key title

ISBN
978-91-7753-014-5 (print)
978-91-7753-015-2 (pdf)

Recipient's notes

Number of pages 87

Price

Security classification

Signature ______________________ Date 2016-10-04

Development and Implementation of a Mouldable Soft Magnetic Composite

Leif Siesing

Faculty of Engineering, Department of Mechanical Engineering

ISBN: 978-91-7753-014-5 (print)
ISBN: 978-91-7753-015-2 (pdf)
LUTMDN/(TMMV-1071)/1-87/(2016)
Printed in Sweden by Media-Tryck, Lund University, Lund 2016

Abstract

Electrical machines, chokes and induction heaters are found in most homes, offices and factories all over the world. They are used to create movement, filtrate the power or to generate heat. A typical unit consist of a coil and a flux conductor material. Some of the materials have been established for over 100 years, while others are only a couple of decades old.

A new flux conductor material has been developed at the Division of Production and Materials Engineering at Lund University. The material is called soft magnetic mouldable composite (SM^2C). This thesis is focused on investigating the potential of this material and lay a knowledge foundation, wherein the material properties and manufacturing process of the material is tested and further developed, as well as the material composition. In order to use the full potential of the material a holistic view of all the materials involved is necessary. Both coil and insulation suitable for the mouldable soft magnetic composite are therefore studied. Tests are performed both on the separate materials, but also together in applications. Several motors and induction heaters were built and tested in different projects.

Results from the work show that by changing from solid copper tubes to litz wire and by using a flux conductor an increase of efficiency from 50–80 % to 98 % is possible. This is due to lower losses in the current conductor and higher flux linkage.

The possibility to mould the soft magnetic composite has interesting potential. It is shown that sensors, current conductors and other soft magnetic materials can be integrated directly into the composite. Also, the technology will provide a good thermal contact between the materials. This is especially important for the current conductor, which is usually the main heat source. A good contact will help conduct away the heat if the device is designed properly.

Other opportunities are opened with the new technology as well. The size of a moulded part has no limit, unlike for other soft magnetic composites that are usually pressed. It is possible to mould parts into almost any geometry, but it is also easy to machine the material if wanted.

Keywords: Soft magnetic composite, Mouldable, Manufacturing, Powder, Thermal conductivity, Permeability, Magnetic loss, finite element analysis.

Acknowledgment

Thank you...

Mats Andersson, for being my supervisor during these years. You have been an inspiration and someone that I can always talk to.

Tord Cedell, for being my co-supervisor during these years. The discussions we had about the understanding of our material developments and different projects have been stimulating, confusing and fun.

Kenneth Frogner, for helping me with anything that I needed and for being my co-supervisor. We had many stimulating discussions about everything from work to travels.

Svante Bouvin, for the help with designing and building test setups and prototypes.

All colleges at the division, for having interesting discussions, being good friends and for the great atmosphere.

Mom and dad, for encouraging my curiosity and childhood needs of knowledge and explanations. You spent many hours helping me study and encouraging me to not give up when I was tired of something. You have been supporting me in my choices of study even though it has not been a straight path.

Anni, the love of my life. Thank you for being there and supporting me even though I often come home and start telling you about my latest escapades at work.

Populärvetenskaplig sammanfattning

Elektriska motorer och induktionsuppvärmingshällar är något som blir allt vanligare i varje hem. Det är också något som blir allt vanligare i industrin. Alla de här produkterna utvecklas hela tiden för att bli energisnålare och billigare. De använder även samma typ av material, mjukmagnetiskt material och en strömledare. Avhandlingen handlar om utvecklingen av ett av de mjukmagnetiska materialen, samt omkringliggande material i form av isolation och elektrisk ledare. Det utreds hur materialen fungerar tillsammans, samt hur tillverkningen påverkar egenskaperna.

En stor del av avhandlingen beskriver hur det mjukmagnetiska materialet har utvecklats och utvärderats. Det är ett kompositmaterial som består av ett järn-kisel pulver som blandas med en epoxi. Detta gjuts i formar istället för att pressas, som är det vanliga med mjukmagnetiska kompositmaterial. Gjutningen gör det möjligt att gjuta mycket större detaljer än vid konventionell pressning. De magnetiska egenskaperna har utvärderats beroende på pulverfraktioner och tillverkningsmetod. Slutsatserna är att en relativt jämn fördelning alternativt bimodalfördelning av partikelstorlekar är bäst, samt att det är bäst att vibrera massan under gjutningen för att få en så hög densitet som möjligt. Materialet har låg relativ permeabilitet, samt låga förluster jämfört med liknande pressade material.

För att verkligen dra nytta av att det går att gjuta det mjukmagnetiska kompositmaterialet så krävs en för-lindad elektrisk ledare. Dessa kan göras på olika sätt, men det är speciellt viktigt i motorer att de är geometriskt stabila. Detta för att få rätt egenskaper på motorn. En form av våg-lindning utvecklades därför, samt tillverkningsprocessen av den. Den har en hög nyttjandegrad av det använda utrymmet, vilket är viktigt i motorer.

Det skapas förluster i form av värme i både det mjukmagnetiska kompositmaterialet och den elektriska ledaren. Därför har även de termiska egenskaperna undersökts för båda materialen. Slutsatsen är att det är viktigt att hålla nere förlusterna i ledaren samt försöka maximera den termiska konduktiviteten i det mjukmagnetiska kompositmaterialet för att hålla nere temperaturen i produkten.

Contents

1 Introduction **1**
1.1 Background 1
1.2 Projects 2
1.3 Objectives 3
1.4 Scope and limitations 4
1.5 Research approach 4

2 Theory and background **7**
2.1 Electromagnetic circuits 7
2.1.1 Induction heaters 7
2.1.2 Motor applications 11
2.1.3 Filtering applications 12
2.2 Electrical wire 13
2.3 Soft magnetic materials 15
2.4 Insulation of litz wires moulded into soft magnetic mouldable composite 18
2.5 Thermal conductivity 20

3 Soft magnetic materials **23**
3.1 Laminated steel 23
3.2 Amorphous alloys 24
3.3 Soft ferrites 25
3.4 Soft magnetic composites 26

4 Measurement methods **27**
4.1 Permeability and iron loss 27
4.2 Comparative material characterisation 28
4.3 Dielectric strength 28
4.4 Dielectric test of coils 29
4.5 Thermal conductivity 31
4.6 Mechanical strength 32
4.7 Fill factor 33
4.8 Density, packing and tap density 33

5 Soft magnetic mouldable composites **35**
5.1 Material composition 35
5.2 Manufacturing methods 37
5.3 Soft magnetic mouldable composite properties 46

6 Winding design for SM^{2}C applications **51**
6.1 Design 51
6.2 Manufacturing 52
6.3 Thermal conductivity of windings 56
6.4 Insulation of winding 58

7 Electromagnetic and thermal multiphysics simulation **63**
7.1 Simulation model 63
7.2 Test setup 64
7.3 Results 65

8 Application cases **69**
8.1 Electrical machines 69
8.1.1 In-wheel motors 69
8.2 Induction heating 70
8.2.1 GreenHeat 70
8.2.2 RaUCH 70
8.2.3 InRoll 72
8.3 Chokes 73
8.3.1 MagChoke 74

9 Conclusions **77**

References **81**

Appended publications

I *Electrical isolation of coils in Soft Magnetic Composite applications*, L. Svensson, M. Andersson, T. Cedell, P. Jeppsson, 4th Swedish production symposium (2011) 510–517.

II *Soft magnetic moldable composites: Properties and applications* , L. Svensson, K. Frogner, P. Jeppsson, T. Cedell, M. Andersson, Journal of Magnetism and Magnetic Materials (2012) 2717–2722.

III *New manufacturing methods for electric motors using different soft magnetic material combinations*, L. Svensson, A. Reinap, M. Andersson, M. Alaküla, 2nd International Electric Drive Production Conference (E|DPC) (2012) 366–372.

IV *Alternative production process for electric machine windings*, L. Svensson, K. Frogner, A. Reinap, C. Högmark, M. Alaküla, M. Andersson, 2nd International Electric Drive Production Conference (E|DPC) (2012) 161–167.

V *Thermal properties on high fill factor electrical windings: Infiltrated vs non-infiltrated*, L. Siesing, A. Reinap, M. Andersson, International Conference on Electrical Machines (ICEM) (2014) 2218–2223.

VI *Investigation of thermal losses in a soft magnetic composite using multiphysics modelling and coupled material properties in an induction heating cell*, L. Siesing, K. Frogner, T. Cedell, M. Andersson, Journal of Electromagnetic Analysis and Applications (2016) 182–196.

VII *Towards energy efficient heating in industrial processes - Three steps to achieve maximised efficiency in an induction heating system*, L. Siesing, F. Lundström, K. Frogner, T. Cedell, M. Andersson, Applied Thermal Engineering, Submitted 2016-07-05.

The Author's contribution to the papers

Below is a short explanation of what the author contributed to in the appended papers.

Paper I

Major part of writing and evaluating was done by the author. Half of the experiments and measurements were performed by the author, and the rest by a co-author.

Paper II

The author performed most of the writing himself with the help of co-writers for proofreading and planning. The experimental work was performed solely by the author, and most of the analysis.

Paper III

The paper was written by the author except for the electrical machine design chapter and the measurements and tests chapter, which were written by a co-author. The paper was planned by the author and the co-authors. The manufacturing of the electrical machines was performed by the author.

Paper IV

Most of the writing was done by the author. The experiments together with the analysis were performed by the author.

Paper V

All of the writing and the planning and experimental work were carried out by the author. The simulations were carried out by a co-author. The co-authors also helped with proofreading.

Paper VI

The planning and experimental work together with simulations and analysis were performed by the author. Most of the writing was done by the author with the help of co-authors.

Paper VII

The planning and most of the writing was done by the author. Chapter 4 "step 1: Using flux concentrator" and "step 3: Mold flux concentrator on the coil" was written by a co-author.

1 Introduction

A significant and increasingly important part of industrial products can be classified as electromagnetic equipment such as electric machines, transformers, induction heaters, and chokes. These devices have been developed for over 100 years, at some periods with very few improvements, but during the last 20 years new materials with enhanced properties have been developed, making it possible to increase energy efficiency in many cases.

For example, new areas for induction heating have arisen, making it possible to replace heating technology based on ovens and furnaces. Another promising area for modern induction heating is in tooling for the manufacturing industry. Here, a combination of reduced cycle times and decreased energy consumption is very attractive. Overall, a future sustainable society and industry will demand much more energy efficient solutions than those available today.

Thus, there is incentive to improve performance and reduce manufacturing costs for inductors and similar devices. In order to accomplish that, a parallel development of both materials and production technology is needed, as well as integration with other technical systems.

1.1 Background

Improvement of a technical system or a functional unit by changing and enhancing material properties can be a complex enterprise, affecting other components in the system as well. Taking induction heating as an example, one measure to increase energy efficiency of an inductor is to replace the commonly used copper tubes with litz wire, which will significantly reduce internal losses, especially at higher frequencies. Even if the losses are reduced, one problem that needs to be solved is the cooling of the litz coil structure. Cooling of a copper tube is obviously done by running a coolant through the tube, but this is not possible with the litz wire. The litz bundle has a relatively poor thermal conductivity, especially in the lateral direction, leading to hotspots if the heat cannot be effectively conducted from these areas. One way to do this is to tightly connect a flux conducting material to the litz structure. The flux conducting material, typically a soft magnetic composite (SMC), has the main function to guide and control the electromagnetic flux in the circuit, thus contributing to an increased overall efficiency, but it could also serve as a conductor of heat if the thermal connection to the litz bundle is good enough. This is one of the motives behind developing a new type of SMC material, a mouldable compound that can be cast and shaped around the litz perimeter. A close contact between litz and SMC material will facilitate a good thermal coupling, but an electric isolation between the two is also needed, putting new demands also on the isolation material. This example demonstrates that a holistic approach is needed when analyzing the consequences of introducing new materials and manufacturing processes in these systems. An additional benefit from having a SMC material that can be directly moulded into a given geometry is the freedom of shape, but also size. In many cases it is beneficial to have isotropic magnetic properties in these structures, thus acquiring true three dimensional properties. Such properties exist for example in pressed SMC structures, but these are often limited in size and complexity in shape. Especially for induction heaters, the freedom to produce large, homogenous SMC structures is a great benefit.

This work has a focus on the developed material, designated as SM^2C, and different methods for processing it, but system integration and the coupling to other components have also been carefully studied.

1.2 Projects

The research in the thesis was performed within several projects, briefly described below. All projects involve development of new concepts for electric motors or induction heaters. Similar materials were used in the projects, as well as similar manufacturing methods, and different aspects of the materials were evaluated in the projects. The author has been developing and evaluating materials in all projects and designs in order to better understand the materials and production methods.

- The GreenHeat project focused on the development of an industrial induction heating unit with enhanced cooling capability, wherein the goal was to combine a highly energy efficient heater with a less complex cooling system based on air cooling. Challenges within the project involved the development of processing and casting technologies for soft magnetic composite (SMC) structures, as well as maximized thermal coupling between coil and flux conductor, among others.

- The DAMIA2 project focused on further developing SMC technology for electric drives, wherein an in-wheel electric motor was designed. The unique possibility to mould three-dimensional shapes from the Soft Magnetic Mouldable Composite (SM^2C) material was utilized in different machine designs, and the benefits from integrating different functional elements into the SM^{2}C structure were evaluated.

- RaUCH was a project where rapid uniform heating and cooling of a tool surface was the primary target. Heating was performed by induction, and one of the main challenges was to achieve uniform heating of a given surface. Further developments of the SM^{2}C material and development of different cooling structures were also tasks within the project.

- The Inroll project aimed to implement induction heating into a food processing unit using a novel and innovative roller design. This would greatly reduce the energy consumption and increase the process performance. A long-term goal was to open up new markets for sustainable technology based on induction heating.

1.3 Objectives

The main objective of this thesis has been to methodically lay a knowledge foundation for the material properties and production process and demonstrate benefits and limitations with a mouldable soft magnetic composite. In relation to this, the following intermediate goals and subtasks have been stated:

- to develop appropriate manufacturing processes for inductors with SM^{2}C and litz wire.
- to develop methodologies for material characterisation of SM^{2}C and litz wire.
- to study thermal conductivity on individual material samples as well as the heat flux of an induction heater unit.
- to analyse limitations and benefits of the studied materials in different application areas.
- to study and analyse the electrical and thermal interaction between material systems involved and to identify critical factors regarding overall functionality such as dielectric strength and thermal management.

1.4 Scope and limitations

The scope of the thesis is very much related to the development of the special mouldable soft magnetic composite. Material characterization and analysis is mainly limited to those material properties valuable for either the design of the finished product or the production.

- The developed SMC material is typically suitable for use at frequencies around 20 kHz. The studied coil materials and configurations have therefore been restricted to litz wire or wire of similar dimensions with the same application range.
- Investigation of coil properties has been limited to study thermal conductivity and to processing of wire bundles.
- The assessment of SM^2C material properties has been limited to measurement of permeability, iron losses and thermal conductivity.

1.5 Research approach

The research presented in this thesis is mainly application driven, see Figure 1. The set demands while developing a specific device, for example an electric motor, will in turn specify the combination of material properties wanted, typically the combination of magnetic, electric, thermal and mechanical properties. Equally important though, are the different aspects involving production of the device, which will greatly influence both functionality and cost, but also interact with which material properties that are possible to reach. The production technology is dependent on, for example, the size, geometry and application of the device. The production technology includes process development, tooling and material composition.

The aggregated constraints and objectives from production and material technology need to be met by research activities in a number of different fields illustrated by the right boxes in Figure 1. Process development and development of a proper tooling setup are of course essential for production development, but equally important is a careful investigation of the influence from different material compositions. Development of measurement methods and strategies has been a major part of the thesis work, as well as the analysis of material characteristics under different conditions. Finally, the interaction between functional units can be analysed through simulation of the device and the application, giving the necessary feedback to the material development performed and also confirming if the set goals for performance are met.

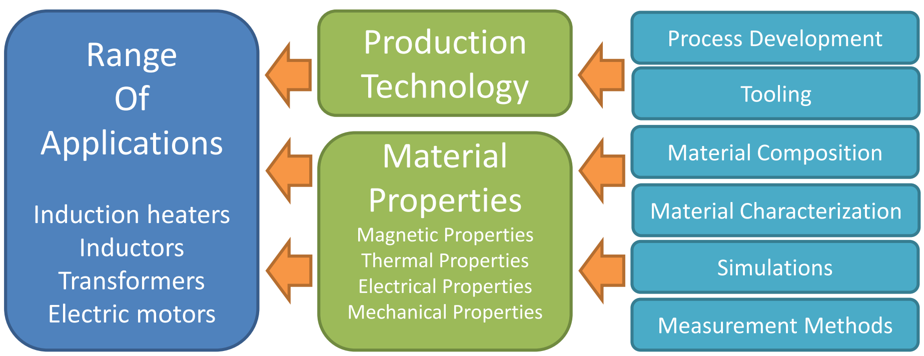

Figure 1: Research methodology used in the thesis.

2 Theory and background

In order to perform a holistic analysis of soft magnetic composite materials, it will also be necessary to involve separate studies of linked systems, typically related to coil configurations and coil materials. This chapter gives a short background to these areas, as well as an introduction to the typical applications and arrangements of the materials.

2.1 Electromagnetic circuits

In this section, a brief overview of electromagnetic circuits or systems is presented in order to contextualize the work performed in the thesis. An electromagnetic system usually consists of three material groups: the electrical conductor, the electrical insulator and the magnetic flux conductor. This work is limited to alternating current applications, which means that the flux conductor should have a relatively low electrical conductivity to avoid excessive eddy current losses.

Studied systems and application typically work in the frequency range of 1–30 kHz. The lower frequencies relates to electric motors with flux conductor built from SMC materials, while the higher frequencies represent induction heating and filtering applications for switched mode power electronics at 15 to 25 kHz.

The coil is essential for all induction circuits, and in most cases a soft magnetic material is used to help guide and control the magnetic flux. Resistive losses will always occur to some degree in the coil material as well as in the soft magnetic material and it is always a balance which properties to improve in order to reduce losses.

The obvious concequence from resistive losses internally within the induction circuit is generation of heat in unwanted areas. In many cases it is therefore necessary to cool the system in one way or another. In some applications the normal unforced convection from the circuit is enough, but in others forced convection in the form of an air flow or a liquid cooling is needed. In the case of induction heaters, heat will be generated in the workpiece and radiate or conduct back to the induction circuit, which makes it necessary to shield the inductor from the environment. In extreme cases it is necessary to cool both the coil and the flux conductor.

2.1.1 Induction heaters

Induction heating can be used to heat electrically conductive materials, mainly metals, but it is also for example possible to heat graphite[1] and carbon fiber composites [2, 3]. The reasons for heating a material are many, and the temperatures typically range from 100 °C to 1000 °C. In some cases minor raise of temperature increase is necessary, for instance when paint is dried or oil from sheet metal forming evaporate [4]. In other cases induction heating is used for melting steel in ironworks or for conducting hardening and tempering operations [5]. Induction heating is a very flexible, effective and versatile way of heating.

The technology can make it possible to locally heat selected parts of a workpiece, which is very attractive in many situations, for example tip hardening of teeth in saw bands. Generally, induction heating has the potential to both boost productivity and improve quality at the same time. Induction is not only a fast way to heat a specific part in an industrial process, the startup time for induction units is also extremely short compared to more conventional heating systems, like ovens and furnaces.

The most common industrial induction heating systems are based on coils from internally cooled copper tubes and generally no flux conductors are used. These is are simple and robust systems, but often show high thermal losses and high magnetic stray fields. The reason for the high thermal losses is that the skin depth of copper at operating conditions is relatively small compared to the wall thickness of the tube, which means that only a small part of the cross sectional area is being used (see section 2.2). Instead, the electric current is concentrated to the outer parts of the tube, which increases the resistive losses.

There are benefits from introducing flux conductors to the coil in order to guide and concentrate the magnetic field towards the workpiece, but also to reduce magnetic stray fields (see section 2.3). In many cases though, soft magnetic materials are not used due to production complexity and maximum limiting temperature.

The shape and size of the induction heater varies depending on the application. For a rod to be heated a simple solenoid coil is the most common and effective shape (see Figure 2c). For a flat surface, spiral coil is more suitable (see Figure 2b). For other setups and configurations a face coil can be employed (see Figure 2a).

Relative motion between inductor and workpiece facilitates even heat distribution, which is a desired feature in many cases. In some applications, such as band heating and heating of rollers, there is a natural movement of the workpiece. In other applications it is possible to move the inductor relative to the workpiece, using for example an industrial robot in order to heat specific parts of a product or to generate uniform temperature [6, 7].

If the heating arrangement requires a stationary setup, even heat distribution is a technical challenge. One way to solve the problem it is to use a travelling wave arrangement [8], which consists of several coils and involves more complicated equipment and control systems.

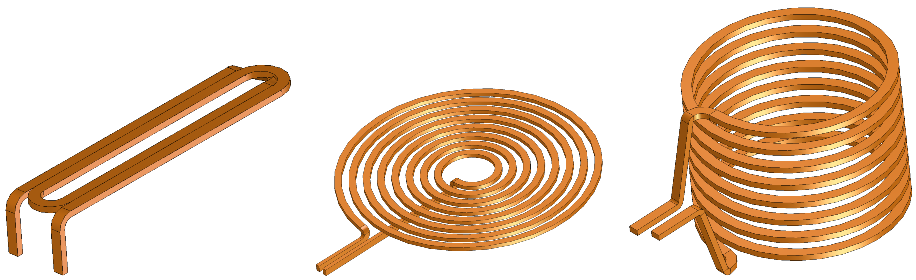

(a) Face coil. (b) Flat spiral coil. (c) Solenoid coil.

Figure 2: Induction heater coil configurations.

As mentioned, the benefits of induction heating are the energy efficiency and the speed of heating compared to traditional heating methods using ovens, IR radiation etc. The coil can have almost any shape and the system can be used for many different materials.

Focusing on energy efficiency it is important that losses in the coil and the flux conductor are kept to a minimum, still with a reasonable system cost. An attractive setup is to introduce suitable litz coil arrangement, while also combining it with a soft magnetic composite material with matching properties regarding for example frequency range. By doing so it is possible to reach an efficiency above 98 % in the induction unit, i.e. from current in the coil to heat in the workpiece, instead of about 50-80 % in a more traditional copper tube inductor coil. There will always appear losses in the frequency inverter and, if used, the transformer, but these are not taken under consideration in this comparison.

The induction heating technology is characterised by non-contact power transfer via an alternating magnetic field typically generated by a solenoid or a face coil. The generated heat in an electrically conducting workpiece is due to induced eddy currents, while for a ferromagnetic workpiece the generated heat is due to a combination of eddy currents and hysteresis losses, where the first of them generally is the dominant source.

Looking at a generic electric circuit (see Figure 3) a number of power loss sources can be identified. The major power losses are related to the frequency inverter, P_Inv, losses in the coil, P_Coil, and the indirect convection and radiation losses from the workpiece, P_Heatflux. For applications where the distance between the inverter and the inductor is significant, the losses in the cabling, P_SWire must be considered when calculating the overall efficiency. In this thesis, the main focus is put on the losses that originate from the heating coil, P_coil.

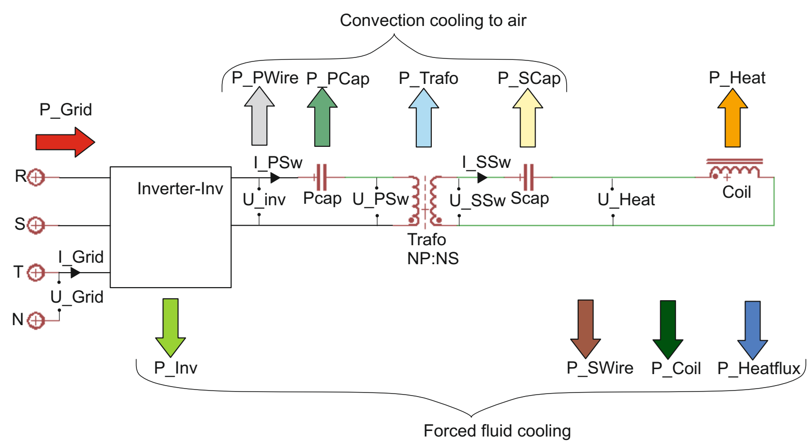

Figure 3: Schematic and loss chart over an induction circuit, including workpiece.

Here, the studied heating coil is a highly efficient face coil designed at the Division of Production and Materials Engineering at Lund University. The heating coil consists of a liquid cooled litz wire moulded within a SMC block. This design optimises the power factor at the same time as it minimises the losses.

The losses, P_Coil, consist of resistive losses, as well as skin and proximity losses in the litz wire, small often omitted dielectric losses between the turns of the coil and hysteresis and eddy current losses in the SMC material. Altogether, these power losses are typically in the order of 2 % of the heating power, for a well designed system with a steel workpiece.

The current can be generated in different ways but usually by a frequency inverter. In some cases a transformer is put after the inverter to match the impedance of the load. Usually also capacitors are connected to the circuit, either in parallel or in series with the inductor in order to compensate for the reactive power. By running the system in resonance the output power is maximised and the reactive power, as seen from the primary side of the transformer, is minimised. To reach resonance either the frequency or the capacitors can be changed to match the inductor.

2.1.2 Motor applications

In an electric motor the generated magnetic field is used for creating a rotating movement. In a permanent magnet motor the magnetic field created by the current in the coil will push or pull in the direction of the magnet. When this force is coordinated for several different magnets and coils a rotating motion is achieved. There are many different designs of motors, some use permanent magnets and some do not, but the basic principle is the same. The design depends on the requirements on the motor such as torque, rotational speed, size and cost.

The most common soft magnetic material in motors is electrical steel sheet laminate, which have high permeability and is relatively inexpensive. These materials are mainly used for low frequency applications, e.g. 50–60 Hz depending on the laminate thickness, due to rapidly increased losses at higher frequencies. A sometimes limiting aspect is that the laminated materials are more or less two dimensional. This means that the magnetic field is preferably guided in the same plane as the sheet. For many machine designs this fact is no major problem, but in some cases isotropic properties is required. A claw pole machine is for example designed so that three dimensional flux paths are the most favourable. Soft magnetic composites or ferrites are isotropic and have the potential to solve the problem in three dimensional applications. However, ferrites will reach saturation too early for most motor applications. Soft magnetic composites will work for some designs, especially at frequencies above 1000 Hz. Figure 4 shows a simulation of an in-wheel motor with a core made from a moulded SMC material.

A limiting factor in electric motors regarding operating conditions is the heat buildup due to power losses in the electromagnetic circuit. These heat losses occur in the windings as well as in the soft magnetic material and locally overheated areas, so called hot spots, is a major concern when designing the motor and choosing the right material configuration. There are different ways to manage the temperature problem. One of the simplest is to increase the copper cross section area in the windings if possible. This measure will in most cases increase cost and size of the motor though. Another approach is to cool the motor with air, water or oil. This can be achieved by directly cooling the coils or the coil ends, but in some solutions

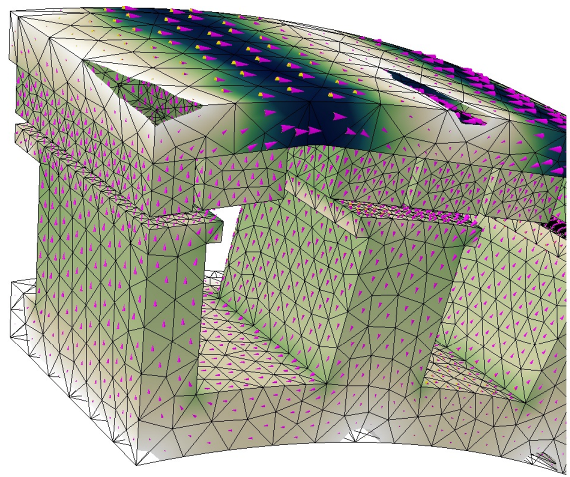

Figure 4: Flux linkage simulation for SM^2C stator core. [9]

the motor is cooled through the soft magnetic material. In the latter case, it is important to have a good thermal contact between the coil and the soft magnetic structure in order to conduct heat away from the coil in an effective manner. A mouldable soft magnetic composite would also allow for easy integration of cooling channels in the flux conducting structure.

2.1.3 Filtering applications

Today, filters for electronics are realised with operational amplifiers, resistors and capacitors. However, before the operational amplifier breakthrough, electronic filters were built with passive components, including chokes. For power electronics, second order filters and higher are built with capacitors and chokes, with common mode and differential mode. For common mode chokes there are special requirements on the core material: high permeability and high frequency performance. Therefore, only the differential mode choke will be addressed in this thesis. The differential mode choke resembles two induction heating face coils pressed together. The losses are similar but the optimisation is made with totally different optimising conditions. For example, the losses should be low at grid and switching frequencies, but higher at switching frequency harmonics so that oscillations are damped. Unwanted high frequency oscillations are devastating for the switching losses of an active front end inverter, for instance. The design of the choke must be done in a way so that either cooling by airflow or liquid cooling can be achieved. In the case where the soft magnetic material is cooled a good thermal coupling between the coil and the soft magnetic material is needed.

2.2 Electrical wire

The most commonly used materials for electrical conductors are copper due to its high electrical conductivity and low contact resistance, as well as aluminum due to its low density and cost, in combination with reasonable low electrical resistivity. Regardless of which of these material that is chosen for a specific application, the so called skin effect, needs to be considered. The skin effect, or rather the skin depth, affects the current density according to Equation 1. The skin depth is decided by the frequency and the material properties. A higher frequency means a smaller skin depth, which often results in an unused conductor area. The skin depth can be calculated by Equation 2. The skin depth is defined as the depth when the current density has been reduced to 1/e ≈ 0.37 of the surface current density. For example, copper has a skin depth of 9.4 mm at 50 Hz, meaning that skin depth is usually not a problem in most low voltage power transfers. At 20 kHz the skin depth is reduced to 0.46 mm. A comparison of the relative current density as a function of the distance from the surface is seen in Figure 5.

$$J(d) = J_S \cdot e^{-d/\delta} \tag{1}$$

$$\delta = \sqrt{\frac{2\rho}{2\pi f \mu_r \mu_0}} \tag{2}$$

With following parameters:

J = Current density [A/m^2]
d = Depth into the material [m]
J_S = Current density at surface [A/m^2]
δ = Skin depth [m]
ρ = Resistivity [Ωm]
f = Frequency [Hz]
μ_r = Relative permeability [-]
μ_0 = Permeability of vacuum [H/m]

The skin depth not only affects the current conductor but also the flux conductor and the workpiece, in the case of induction heating. This means

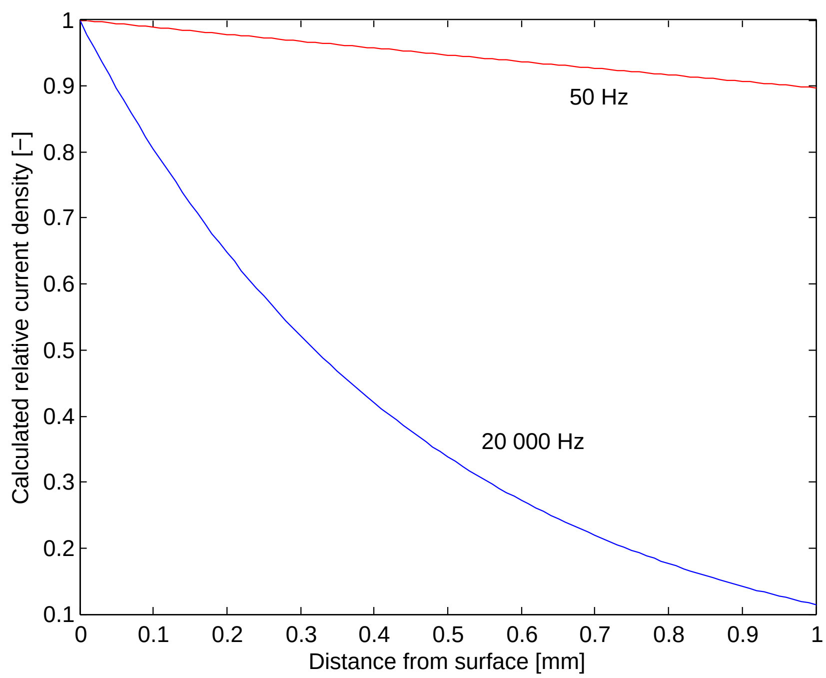

Figure 5: Calculated relative current density as a function of the relative field penetration depth using Equation 1 and 2.

that the frequency must be matched with the proper conductor thickness and material, flux conductor thickness and material, and workpiece thickness and material for each individual induction circuit.

For the induction heater high losses due to the skin effect are desirable in the workpiece, while it is preferably minimised in the current conductor and in the flux conductor. The different materials involved thus need different properties to achieve this. The current conductors' strand cross sectional area should be adapted to the frequency used in the application. This is performed by dividing the conductor into multiple individually insulated strands, twisted so that each exhibits the same high frequency properties. This wire is called litz wire and typically has a strand diameter of 0.15–0.2 mm for 20 kHz applications, which is common for most induction heating cases studied in this work.

The proximity effects also have to be considered when designing induction heating circuits. A magnetic field is created when an AC is flowing through an electrical conductor, and this will influence other electrical conductors in its close vicinity by electromagnetic induction. The alternating magnetic field will induce eddy currents in the adjacent electrical conductor, thereby influencing the current distribution. A similar phenomenon will occur in induction heating when a workpiece is involved. The current will then be concentrated near the workpiece and thereby increase the losses. An example of this can be seen in Figure 6, which shows a planar simulation with two parallel solid current conductors, carrying the same amount of current traveling in the same direction.

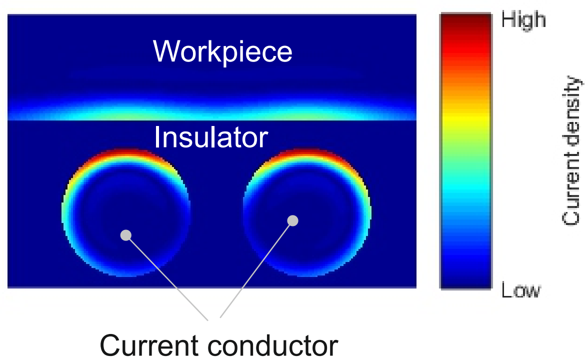

Figure 6: Simulation in FEMM of high frequency current (20 kHz) in solid 6 mm diameter conductors showing skin and proximity effects. The colour scale is linear [10].

The proximity effect in the current conductor can be minimised by using litz wires with proper dimensions. In Figure 7 a simulation with two parallel litz conductors is illustrated, where the current is traveling in the same direction.

2.3 Soft magnetic materials

The main purpose for a flux conductor material is to guide and control the magnetic flux and to increase the magnetic flux density where needed. The benefit from this may be a higher torque in an electric motor, or a higher and more concentrated flux that can be guided to the workpiece in an induction heater to generate a higher power density. The magnetic field created by the current in the coil aligns the structure of the flux conductor. In an AC application the magnetic field will continuously shift directions and the structure will follow. The soft magnetic material will return to a

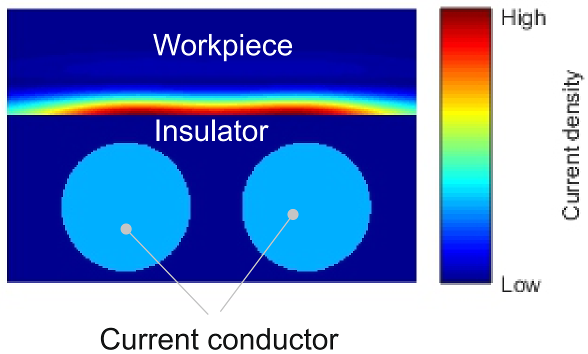

Figure 7: Simulation in FEMM of high frequency current (20 kHz) in 6 mm diameter litz wires with strand diameter 0,2 mm showing no skin nor proximity effects. The colour scale is linear [10].

non-magnetised state when the current is turned off.

The relationship between ampere turns, magnetic flux, the magnetic reluctance and permeability is described by Equation 3 and 4.

$$R = \frac{F}{\Phi} \tag{3}$$

$$R = \frac{l}{\mu_0 \mu_r A} \tag{4}$$

With following parameters:

R = Reluctance [1/H]
F = Total current, sometimes called the magnetomotive force [A]
Φ = Magnetic flux [Wb]
l = Length of the magnetic path [m]
μ_0 = Permeability of vacuum [H/m]
μ_r = Relative permeability [-]
A = Cross-section area of the magnetic circuit [m^2]

Every time the magnetic field is switched the structure changes and this requires energy, which is the reason why hysteresis loss occurs. The size of the loss varies for different materials and can be described by a B-H curve (see Figure 8). The relationship between B, H and permeability can be seen in Equation 5. The permeability is a constant of proportionality that exists between magnetic induction and magnetic field intensity.

$$B = \mu_r \mu_0 H \tag{5}$$

With following parameters:

B = Magnetic flux density [T]
μ_0 = Permeability of vacuum [H/m]
μ_r = Relative permeability [-]
H = Magnetic field strength [A/m]

H_C in Figure 8 is the coercivity force and B_r is the magnetic remanence, parameters that are primary related to hard magnets but also gives an indication of the magnitude of the hysteresis losses. The magnetisation loss is calculated by integrating over the contained surface inside the B-H curve.

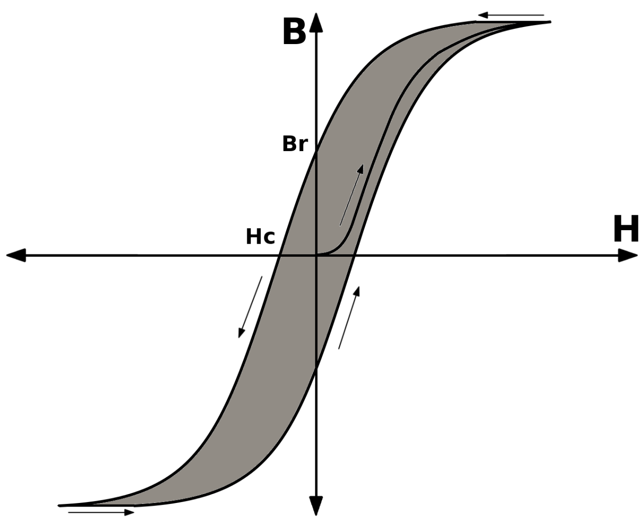

Figure 8: Principal magnetisation curve with hysteresis.

There is only a practical limitation to how high H-field that can be applied, but the B-field will reach an asymptotic value. This effect is described as saturation, and above the value of saturation the relative permeability will converge towards 1. The saturation is an important property when choosing a flux conductor.

A common way to characterise the relationship between frequency and loss is the Steinmetz equation, Equation 6:

$$P = kf^{\alpha}B^{\beta} \tag{6}$$

With following parameters:

P = Power loss density [W/m^3]
k = Fitting coefficient [-]
α = Fitting coefficient for frequency dependence [-]
β = Fitting coefficient for flux density dependence [-]
f = frequency [Hz]
B = Peak magnetic flux density [T]

The coefficients, which must be fitted using measured data, lose accuracy if the frequency range is too wide. Another disadvantage with Equation 6 is that it is only valid for sinusoidal waves. However, this can be solved by dividing a complex current waveform to a composite waveform consisting of current amplitudes at discrete frequencies.

There are many different types of flux conductors and soft magnetic materials. For DC applications a solid iron flux conductor can be used, but for AC applications the losses would be too high, mainly due to eddy currents. Therefore, there are three main types of composite flux conductors commonly used, based on sheet, powder or wire. Which one to choose depends on the application and frequency. Different applications will have different requirements in form of losses, saturation, permeability, and manufacturability.

2.4 Insulation of litz wires moulded into soft magnetic mouldable composite

Most of the text in this subsection is transferred with minor modifications from Paper I [11].

Insulation materials are usually assessed in terms of dielectric strength. Dielectric strength is defined as the maximum voltage required to produce a electric breakdown through the material, expressed as Volts per unit thickness [V/m]. This means that the higher the dielectric strength and resistivity of a material the better the quality as an insulator. There are different factors that affect the dielectric strength of a polymer material: thickness of the material, operating temperature, frequency and humidity. There are a few test methods to determine the dielectric strength, the most readily used places the material between two copper plates which are Energised. What differs between methods is how the voltage is regulated. One test method starts with 0 volts, and then voltage is increased at a uniform rate until decomposition occurs in the specimen. Another alternative is to increase the voltage within predefined intervals.

A material can show different dielectric strength due to possible defects from the coating process, e.g. small air bubbles or various defects, which will decrease the total dielectric strength. Air has a lower breakdown or arc strength than the coating material does. In Figure 9 a small defect can be seen in the form of a disc of thickness t located in a coating material of thickness d. In the analog circuit, the capacitance C_c is that of the cavity, the capacitance C_b is that of the material in series with the cavity, and C_a is the capacitance of the rest of the material [12].

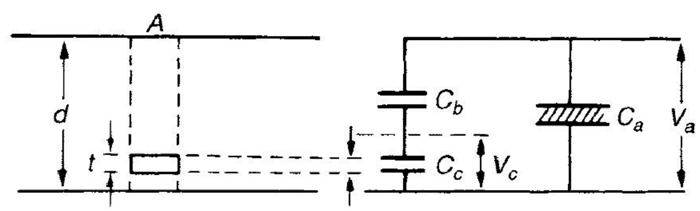

Figure 9: Electrical discharge in a cavity and its equivalent circuit [12].

In reality, most air cavities are spherical. When applying coating on a solid material, the wetting tendency is a factor to take into consideration. According to the Young equation, Equation 7, solid vapour γ_{SV} interface, surface energy of the liquid vapour γ_{LV}, and surface energy of the solid liquid γ_{SL} interface give the surface energy and contact angle θ_e.

$$cos\theta_e = \frac{\gamma_{SV} - \gamma_{SL}}{\gamma_{LV}} \tag{7}$$

Another important factor is that of the surface characteristics of the solid such as its roughness and its porosity. The first of these is dependent on the combination of the coating material and the solid material, whereas the second is dependent upon the handling and the treatment of the material. Theoretical studies, as well as experiments on idealised rough surfaces, show that peaks and grooves act as energy barriers to the movement of a drop

[13, 14]. Drops may "jump" when the contact angle exceeds a certain limit. This means that when a drop passes over a top it might entrap an air bubble (see Figure 10) [15].

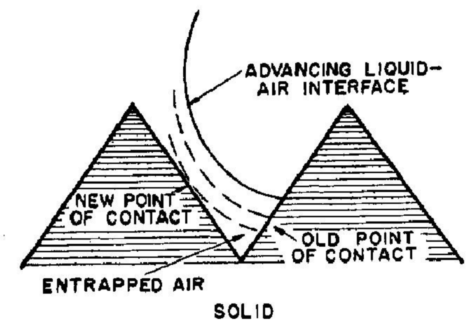

Figure 10: As a liquid advances over a solid, the liquid makes contact with the opposite face and air is entrapped beneath the drop [15].

The air bubble may then be trapped in the coating and, as it cures or dries, the coating also gets thinner through excess coating material dropping off. If the coating gets thinner than the bubble it may burst and create a pinhole that becomes a weak spot in the protective layer. The sequence of breakdown of a sinusoidal alternating voltage is shown in Figure 11. V_a is the voltage applied across the material, the dotted line shows the voltage that would appear if the material did not break down due to the defect. When V_c reaches V+, a discharge takes place, with the voltage V_c collapsing. The voltage then starts to increase again across the defect to reach the level V^+ and collapses again. This can occur several times as the voltage increases, as well as when it starts to decrease and reaches V^-. The discharges in the cavity may damage the coating around it due to both the rise in temperature and chemical degradation of the material.

2.5 Thermal conductivity

It is important to know the thermal conductivity in materials used in induction heaters, chokes and motors. This is due to the high losses in the current conductor and depending on the design, also in the soft magnetic core and for induction heaters in the workpiece. It is therefore important to perform a good thermal design in order to conduct away the heat. The thermal conductivity can be measured, theoretically calculated or simulated in a FEA. The measurement method used is described in section 4.5. Mea-

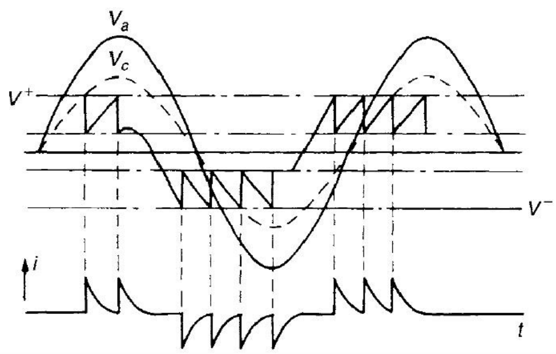

Figure 11: Sequence of cavity breakdown under alternating voltages [12].

suring is only used for evaluation of already produced materials, but it is sometimes important to be able to predict the material properties. This applies particularly to coils. The thermal conductivity of a coil structure is very dependent on the fill factor, and thereby the manufacturing method. A change in fill factor from 0.5 to 0.75 can change the thermal conductivity on a non-infiltrated coil structure by three times in the lateral direction [16]. The thermal conductivity can be calculated in a two-dimensional thermal simulation tool, such as Finite Element Method Magnetics, considering a one-dimensional heat flow. The Hashin and Shtrikman approximation [17], Equation 8, can be used to calculate the thermal conductivity of a composite consisting of two materials. In order to use the approximation for more than two materials a rule of mixture can be used for the two materials with the most similar thermal properties.

$$k_e = k_p \frac{(1+\vartheta_{cu})k_{cu} + (1-\vartheta_p)k_p}{(1-\vartheta_{cu})k_{cu} + (1+\vartheta_p)k_p} \tag{8}$$

With following parameters:

k_e = Effective thermal conductivity [W/mK]
k_{cu} = Thermal conductivity of copper [W/mK]
k_p = Thermal conductivity of potting compound [W/mK]
ϑ_{cu} = Volumetric fraction of copper [-]
ϑ_p = Volumetric fraction of potting compound [-]

3 Soft magnetic materials

This chapter is transferred with minor changes from Paper II [18].

Soft magnetic materials must confine and guide a magnetic field in an optimal way, given the design and function of the electromagnetic unit [19]. The desired properties are mainly related to this basic functionality and can be designated magnetic properties, including permeability, hysteresis losses, eddy current losses, saturation, dielectric strength, magnetoelastic properties, and anisotropy. Permeability and losses are of course critical in many applications, but anisotropy is an important property when comparing laminates with soft magnetic composite materials [20]. Magnetoelastic properties determine the potential or risk of vibration and high noise levels.

Other important properties, including thermal conductivity, temperature resistance, mechanical strength, cost, and manufacturability, can be very important depending on the application. High thermal conductivity and high temperature resistance can be beneficial in choke applications, whereas mechanical strength is important in rotating machine parts.

3.1 Laminated steel

Laminated steel cores of various silicon contents, usually 1–3 %, are built up by stacking electrically insulated steel sheets, so-called electrical steel, giving them relatively high permeability in combination with relatively low losses at lower frequencies. The steel can be either hot or cold rolled depending on the desired material properties, but cold rolled steel is more commonly used since its magnetic properties can be better controlled. Grain-oriented steel has higher permeability and lower losses than non-grain-oriented steel, measured parallel to grain direction [19]. To increase the resistance between layers and thus reduce eddy current losses, every sheet is coated with a suitable non-conductive material, either organic or inorganic. The insulation layer insulates not only against currents but also against heat transport. In a non-grain-oriented steel, that is NO 20 grade, the coefficient of thermal conductivity, k_{th}, is 28 W/mK in the lamination plane, but is only 0.37 W/mK normal to the lamination plane [21]. Cores are produced in various lamination thicknesses, typically 0.15–0.6 mm, but thicknesses down to 0.05 mm do exist [22]. Such steel cores can be manufactured quickly and cheaply, but the winding is more or less easily applied depending on the design. Alloying steel sheets with up to 6.5 % silicon will produce a material with higher resistivity, and therefore producing lower losses due to eddy currents. Electrical steel with 6.5 % silicon content will have zero magnetostriction, which apart from being soundless also minimises the magnetisation losses. Increasing the silicon content to 6.5 % makes the material harder and more brittle, and at a level of 4 % silicon or higher, the steel cannot easily be rolled or plastically deformed. To achieve silicon levels over 4 %, extraordinary methods such as the PVD processing of pre-rolled sheets must be employed [23] with a great impact on material cost. Laminated steel cores are used mainly in low-frequency transformers and electric motors.

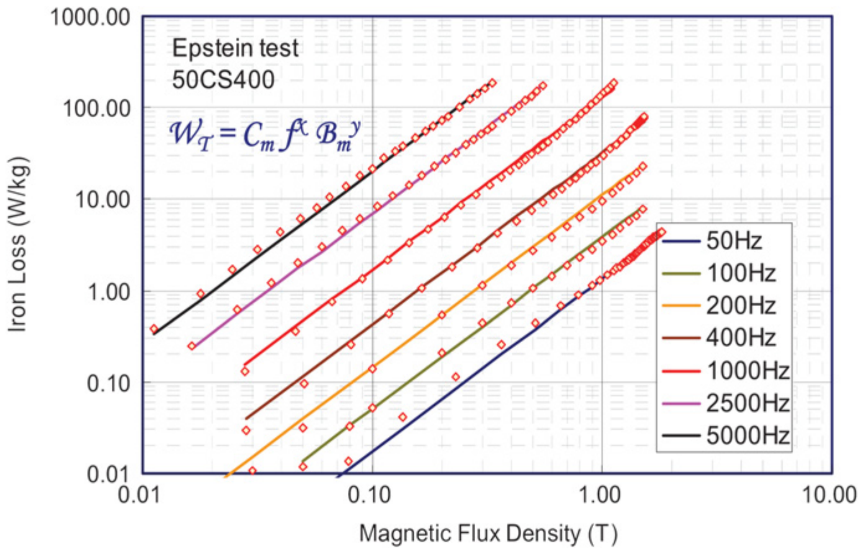

Figure 12: Iron losses in laminated steel sheets made of 50CS400 grade, non-grain-oriented electrical steel suitable for the high volume production of rotating electrical machines [24].

The relative permeability of laminated silicon iron is typically in the range of 6000–18,000 @ DC. The power losses of a representative silicon-alloyed electrical steel are presented in Figure 12. A numerical regression of the measured values according to the Steinmetz equation, Equation 6, yields the following predictive result in Equation 9:

$$P = 26.2 f^{1.88} B^{1.53} \tag{9}$$

3.2 Amorphous alloys

This group of rapidly solidified alloy materials is also known as metallic glass. These materials are produced by rapid solidification at cooling rates of approximately a million degrees Kelvin per second. This means that the atomic structure resembles that of glass, a non-crystalline frozen liquid. Because of the rapid cooling, the material must be very thin, usually 20–30 μm [25, 26, 27].

There are two main groups of amorphous alloys: iron-rich magnetic alloys use cheap raw material and have the highest saturation magnetisation of the amorphous alloys, while the cobalt-based alloys have very low or zero magnetostriction, as well as the highest permeability and the lowest core losses of the amorphous alloys. All amorphous alloys have high electrical resistivity and are very thin, meaning that they have acceptable eddy currents at high frequencies despite their extremely high permeability [25]. The relative permeability of amorphous materials is typically in the range of 35,000–600,000 @ DC.

Measuring the properties of Metglas 2605SA1 iron-based alloy, 25 μm thick, from 400 Hz to 8 kHz yielded the Steinmetz coefficients $\alpha = 1.44$, $\beta = 1.68$, and $k = 2.3$ [28]. This alloy has many application areas, including industrial and power transformers, electric filters, current sensing, motors, and induction heaters.

3.3 Soft ferrites

Soft ferrites are soft magnetic materials manufactured from various oxides, in other words iron oxide commonly combined with nickel, zinc, and manganese oxides. The oxides are mixed, pressed together and sintered. The material is then milled to a fine powder and pressed and sintered again to form the final shape [25]. This means that the material is quite brittle and can easily break if not handled carefully. In addition, the temperature stability is poor, making careful thermal engineering necessary. The thermal conductivity is typically 4 W/mK. The relative permeability of soft ferrites is typically in the range of 500–5000 @ DC.

The Steinmetz coefficients for the Magnetics F soft ferrite material at 25°C are $\alpha = 1.06$, $\beta = 2.85$, and $k = 369.5$. Ferrites, on the other hand, have low losses [29], and their operating frequencies generally range from 1 kHz to well over 1 MHz [22]. Therefore, soft ferrites are used in electric filters to absorb high frequencies in EMI suppression, induction heaters and transformers.

3.4 Soft magnetic composites

This material is manufactured by pressing insulated powder into its final shape [30]. The insulation coating is an important feature of SMC materials, because it eliminates the so-called bulk eddy currents, therefore reducing the losses. Pressing deforms the powder, resulting in higher permeability, higher magnetisation losses and the risk of higher losses due to damaged insulation layers. Because of the isotropic properties of the material, new designs are possible [31] and can even be used at frequencies as high as 200 kHz. The powder used usually consists of pure iron, iron alloyed with silicon, or an alloy of iron, silicon and aluminium, so called Sendust [19]. Some SMCs are heat treated to reduce losses [25].

The relative permeability of SMCs is typically in the range of 50–500 @ DC. For Somaloy 500 compacted at 800 MPa, the Steinmetz coefficients are $\alpha = 1.09$, $\beta = 1.8$, and $k = 612$.

The mechanical properties of SMCs, especially the toughness, are fairly poor but not as poor as those of the soft ferrites. Edge defects after machining are quite common. The thermal conductivity is typically 5–20 W/mK. The material is used in electric motors and inductors. The high pressures required when forming the powder into solid bodies limits the size and the shape of the SMC parts.

4 Measurement methods

Measurement technology has played a very important part when studying, developing and analysing the soft magnetic materials in the thesis. Several of the measurement methods described are well known, but has been adapted to best suit the studied materials and the level of accuracy needed.

4.1 Permeability and iron loss

When measuring permeability and magnetic losses on a soft magnetic material, e.g. a soft magnetic composite, a toroid shape is preferred as it has well defined electromagnetic behaviour with low magnetic leakage and small gradients of the magnetic field. The toroid is wound with two separate windings; a primary and a secondary. Applying a current on the primary winding will induce a voltage change across the secondary side.

$$\varepsilon = -N\frac{d\phi}{dt} \tag{10}$$

$$N \cdot I = \oint_C H dl \tag{11}$$

According to Faraday's law of induction, Equation 10, the magnetic flux, ϕ, is calculated through integration of the induced voltage, ε. In accordance with Ampère´s circuital law, Equation 11, the magnitude of ampère-turns, $N \cdot I$, is given by the summed total of the magnetising field over the mean magnetic circumference, C, of the specimen. Through the constitutive relationship in Equation 5 several different magnetic properties can be determined, most importantly μ_r and hysteresis losses over an electrical period.

A waveform generator, controlled from a computer running LabVIEW, produces an input reference signal to a current controlled power amplifier, AE Techron 7796. The current and induced voltage measurement signals are collected with a data acquisition system also controlled by LabVIEW. By having the LabVIEW program to generate a current and frequency sweep, it is possible to retrieve the Steinmetz coefficients by utilising the resulting data in least squares fitting. Figure 13 give an illustration of the setup.

In the measurements a standardised geometry, inner diameter 45 mm, outer diameter 55 mm, and height 5 mm on the toroids are used. The number of turns on the primary and the secondary windings are 60 turns each. The primary wire has a cross section of 1 mm^2 and the secondary 0.2 mm^2. The reason for using different dimensions on the wires is that more turns generates a more amplified signal, reducing the sensitivity of disturbances,

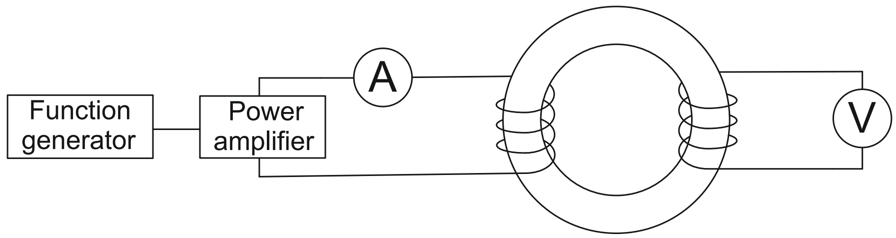

Figure 13: Setup for measuring permeability and loss on toroids [18].

and it is only the primary wire that is exposed to a high current. It is therefore motivated to use different wire diameters so that more turns can be fitted on the toroid.

4.2 Comparative material characterisation

The properties of soft magnetic composite materials depend to a large extent on the input powder material such as material type, size distribution and coating etc. To produce soft magnetic composites and to prepare test objects is a time consuming process, so being able to make a fast screening of dry powder is beneficial. By filling a glass cylinder with the powder mixture and compact it, the resulting losses and magnetic permeability can be estimated. It is a non-destructive testing method, so the powder can be reused.

The characterization is performed using an inductive method, where a solenoid is placed around the test sample and the inductance and resistance are measured at a certain frequency, typically 25 kHz. Measurements are performed multiple times on each sample, and the best value is selected as the most representative result. Experiments have shown a clear correlation between the screening results and the values obtained from the composite materials based on the same powder, even though a reliable relation cannot be determined. This method has played an important role to find interesting combinations of powder fractions to be tested on real samples.

4.3 Dielectric strength

Dielectric strength is the maximum electric field that a material can withstand without breakdown. There are different ways of measuring dielectric breakdown, as well as how to define a dielectric breakdown. The principle used in this work is to successively increase the DC voltage over the sample in a specific pattern where a higher number represents a higher voltage: V1, V2, V1, V2, V3, V2, V3 etc. (see Figure 14).

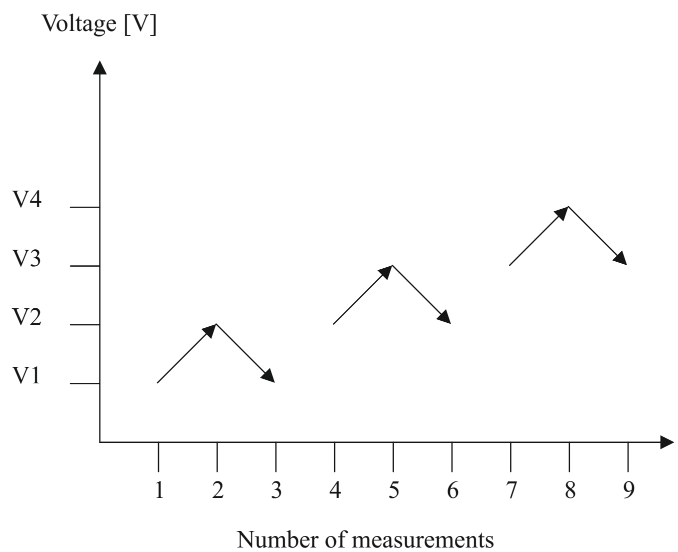

Figure 14: Schematic Figure over the voltage pattern used for dielectric breakdown tests.

This is performed until a breakdown condition occurs, which is defined as when the leakage current through the sample exceeds 10 mA or if the leakage current for the first and second measurement of, for example, V2 deviates more than 30 %. Then V2 is considered the maximum voltage. The sample is clamped in a vice with the teeth insulated from each other, and the surface where the sample is mounted is covered with a braided tin-plated copper ground strap for good contact between sample and measuring equipment. Samples are normally rods with the diameter 16 or 20 mm and a length between 10 and 20 mm. Different lengths are used in order to optimize measurement resolution within the measuring equipment's limitations. For controlling the output voltage and collecting the data a LabVIEW program has been developed.

4.4 Dielectric test of coils

This section is transferred with minor changes from Paper I [11].

The metal powder in the studied SMC materials has a diameter from 10 μm up to 500 μm. This means that the powder has the ability to penetrate almost any pinhole or cavity. The test method must thus be able to emulate this in order for accurate results to be obtained. By experimenting, the research group found that placing the coil in a water bath was quite similar to the conditions while moulding a SMC core around it. Except for defining if the insulation is insufficient, this make it possible to sometimes determine where the electrical insulation coating is damaged, through the bubbles that are created by the leaking current or through the occurrence of small electric arcs. The method for testing the coating was to connect one end of the coil to a variable power supply, and to use accurate current and voltage meters (see Figure 15). It is important to place the non-insulated ends of the coil above the water level so that it will not short circuit through the water. Connecting the negative terminal from the power supply to a conducting container and then placing the coil in the container filled with tap water makes it possible to measure the leakage current. The power supply is programmed to turn off if the current exceeds 10 mA. The voltage is increased incrementally, measurements being made at 100 V steps, starting at 0 V. According to the directive IEC 61558, the leakage current from all the coils in the machine has to be lower than 10 mA at 3 kV DC during one minute.

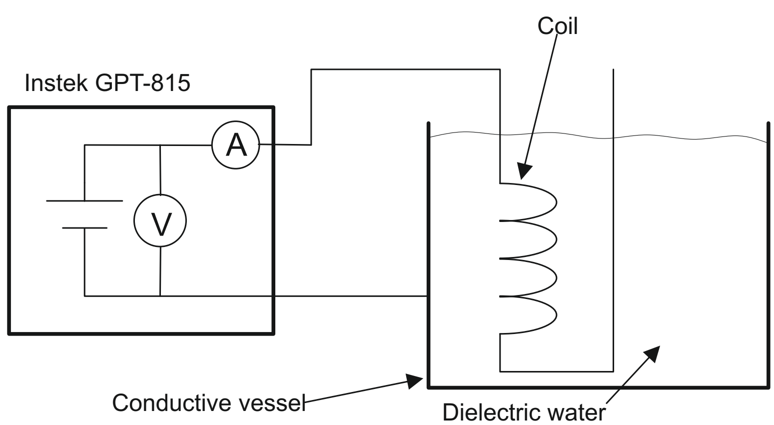

Figure 15: Schematic over the test equipment for dielectric test of coil.

4.5 Thermal conductivity

This section is transferred with minor changes from Paper VI [32].

There are numerous ways to measure thermal properties of a material. In this study the transient plane source method was used. The reason for choosing this method is that it is possible to measure isotropic samples, as well as anisotropic. The equipment used was a TPS 2500 S from Hot Disk AB, and chosen due to the possibility of measuring using short pulses, which allows measurements on small samples. The properties measured in the equipment is thermal conductivity [W/mK], thermal diffusivity [mm^2/s] and specific heat [MJ/m^3K] [33]. The sensor consists of an electrically conducting pattern in the shape of a double spiral, which has been etched out of a thin nickel foil. The spiral is sandwiched between two thin sheets of an electrically insulating material (Kapton) (see Figure 16).

Figure 16: Kapton sensor used for measurements [32].

When performing a measurement, the sensor is placed between two pieces of the sample. Both samples must have a flat surface at least twice the diameter of the sensor. A current is passed through the double spiral. The current needs to be strong enough to increase the temperature of the sensor with several degrees over a defined measurement time. At the same time, the resistance is measured and recorded as a function of time. This measuring technique makes it possible to use the spiral as both sensor and heating element. The thermal conductivity equation used in the software assumes that the sample is infinitely large. Thus, it is important to only use data collected before the boundaries influence the measurement.

The thermal properties has been measured for both windings and SM^2C using this technique. In the tests on the windings the 5501 sensor (6.403 mm in radius) was used. This sensor was recommended from the chief science officer at Hot Disk AB due to the size of the sample and the anisotropic characteristic. The 5501 sensor has also mainly been used on the SM^2C material. Because the winding samples were anisotropic, the volumetric specific heat [MJ/m^3K] needed to be known, Equation 12.

$$C_v = C_{v,Cu}\vartheta_{Cu} + C_{v,pi}\vartheta_{pi} + C_{v,air}\vartheta_{air} \tag{12}$$

With following parameters:

C_v = Volumetric specific heat of composite[MJ/m^3K]
$C_{v_{C}u}$ = Volumetric specific heat of copper [MJ/m^3K]
$C_{v_{C}u}$ = Volumetric specific heat of air [MJ/m^3K]
ϑ_{Cu} = Volume fraction of copper [-]
ϑ_{pi} = Volume fraction of polyamide-imide [-]
ϑ_{air} = Volume fraction of air [-]

4.6 Mechanical strength

A three-point bending test is used for testing mechanical strength such as flexural stress and flexural modulus. Samples used for this measurement are rods with a diameter of 16 or 20 mm. The supports are set with 70 mm spacing, which means that the sample must be at least that long. The support and loading points have a radius of 10 mm. A schematic figure can be seen in Figure 17.

The flexural stress is calculated according to Equation 13 and the flexural modulus according to Equation 14.

$$\sigma_f = FL/(\pi R^3) \tag{13}$$

$$E_f = L^3F/(12\pi R^4 d) \tag{14}$$

with following parameters:

σ_f = flexural stress at midpoint [MPa]
E_f = Flexural modulus of elasticity [MPa]
F = Load [N]
L = Support span [mm]
R = Radius of the beam [mm]
d = Maximum deflection of the centre of the beam [mm]

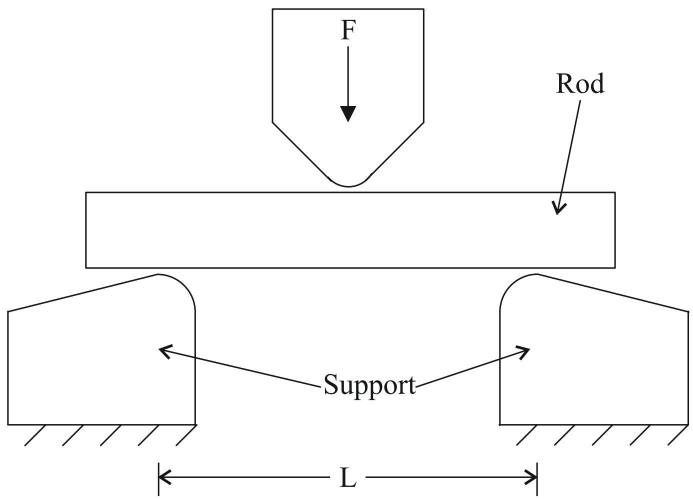

Figure 17: Schematic figure over the three point bend fixture.

4.7 Fill factor

The fill factor of a copper winding or coil is an important factor when analyzing the electromagnetic systems functionality. The fill factor is not however easily predicted or calculated for compressed litz coil. The most accurate and stable method is to study a cross section of a cut sample in a microscope and make use of the contrast between the copper material and the matrix. By using image analysis software routines, the relative amount of copper can be calculated. This procedure is repeated for a number of representative areas of the sample in order to get a valid average value. A microscope picture of two typical samples used in the measurements can be seen in Figure 18.

4.8 Density, packing and tap density

Instead of measuring the permeability on wound toroids, density can be used to compare samples produced with different methods or with different powder fractions. It can be shown that the density has a well-defined relationship to the permeability, see Figure 20. The volume is measured by using Archimedes principle. It is a very accurate method of measuring volume, performed by lowering the specimen into a container of destilled water that is placed on a scale. It is important that the specimen is suspended

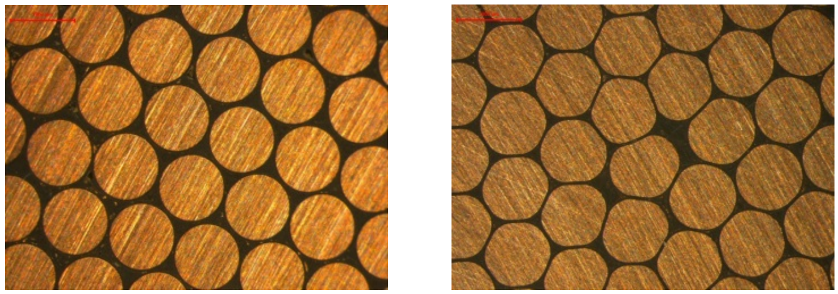

(a) 74 % fill factor. (b) 82 % fill factor.

Figure 18: Microscope picture of the polished surface of compressed copper wires with the diameter of 1 mm [16].

freely in the water without touching the walls or bottom. It is also important that the specimen is kept still so that the water is not moving during the measurement. The weight registered by the scale is equal to the volume of water that the specimen displaces. This means that 1 kg is roughly 1 dm^3 at room temperature. The dried specimen is then weighed without the water, at which point the density can be calculated by dividing the weight by the volume. The volume of the wire used to suspend the specimen from is small enough to be neglected when measuring the displaced water. The scale used has an accuracy of 0.01 g, and all samples weigh between 12 and 130 g.

The particle packing of the iron-silicon powder is calculated by using the measured density and the known density of the iron-silicon and the epoxy. The amount of air bubbles trapped in the composite is considered to be negligible; however, the amount of coating is not. The coating thickness is 6–8 μm, which on a 250 μm thick grain means adding 15 % of its volume without changing the permeability. This means that there is a substantial amount of coating in the composite. All presented data in the following diagrams are compensated for this factor, except for the data in Figure 24.

Tap density is a way of quickly screening the bulk geometric properties of the powder. This is done in order to save time and material when many different powder configurations are to be tested. It is performed by pouring the powder into a measuring cylinder that is mounted on a sieve. The sieve is vibrated for two seconds and the volume is measured. The tap density can then be calculated using weight and volume of the powder.

5 Soft magnetic mouldable composites

The soft magnetic mouldable composite, denoted as SM^2C, is a material developed at Lund University at the Division of Production and Materials Engineering [18]. The material is processed through moulding, unlike to most other SMC materials that are pressed. The material has been developed for use in chokes and induction heaters [34, 35, 36, 37, 38, 8]. It has also been tested for electric motors [39, 40, 41, 42, 43, 44, 9, 45, 46].

5.1 Material composition

The material consists of gas atomised iron-silicon powder mixed with a binder. Gas atomisation is used because it produces spherical particles to a reasonable cost, which is crucial for the moulding process to achieve a high particle packing. The binder is an epoxy resin with low viscosity and good wetting properties to metals. The wetting properties are important because it acts as an insulator between the particles and provide mechanical strength. The powder used in this thesis is a 6.5 % silicon alloyed iron. The reason for choosing this composition is the high permeability, high resistivity close to zero magnetostriction, low DC magnetisation losses and, in general, stable properties. The permeability is highly dependent on the particle packing, and several mixes of particles of different sizes are evaluated. The particle size span from 10 to 500 μm, and is chosen for two reasons: it is possible to get it produced at reasonable cost, and it is reasonable suitable for the frequencies used.

Powder from a single batch was sieved into different fractions using a laboratory sieve. The different fractions were mixed in different combinations to find the best powder particle size distribution. The packing and size of the particles significantly affects the magnetic properties [47]. Particle size is also a factor when adapting the SM^2C material for different frequency ranges, due to eddy currents. If particles of only one size would be used, a packing of 74 % is the theoretical maximum [48]. However, when taking into account that the spheres are packed randomly only a packing of 63 % is possible [49]. In theory the best strategy is to mix small particles with large particles, so that the small particles can fit in the space between the larger ones. Even smaller particles can be fitted between the small particles, and so on. In reality it is impossible to manufacture a powder with these characteristics. It is possible to extract particles from the produced powder and then mix it according to theory, but huge amounts of powder would have to be wasted or used as raw material in a new batch. Another possibility is to remove only a fraction in the middle to achieve something similar to a bimodal distribution. If such a size distribution would be possible to obtain directly from the powder production or with smaller modifications, it would be much more cost effective. The particle size distribution for different tested mixing relations are shown in Figure 19.

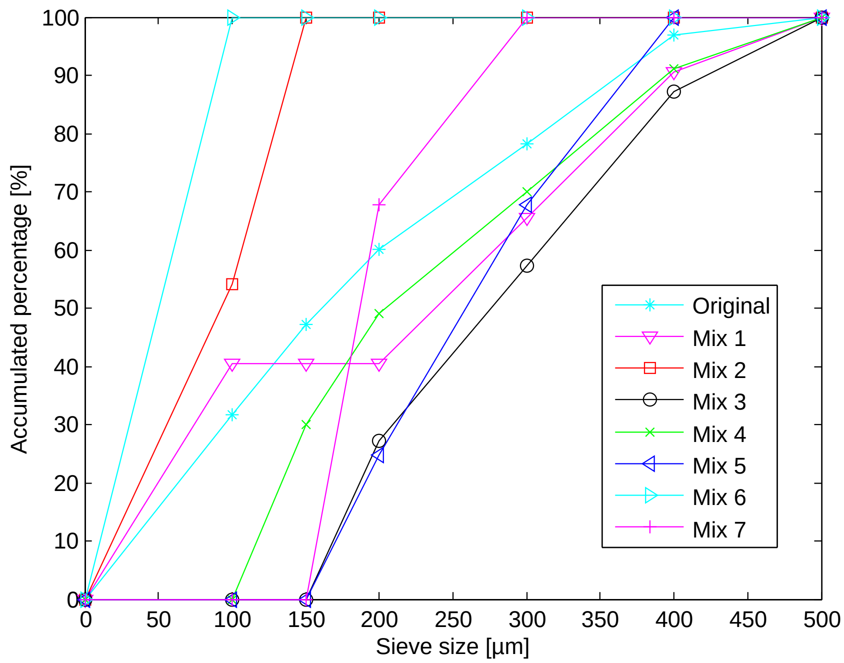

Figure 19: Particle size distribution for different mixing relationships.

The powders are measured by using a comparative material characterisation method, see section 4.2. This will only show the relationship of permeability between the measured powders in order to identify which ones to perform further studies on. Inductance measurements for the different powders from Figure 19 are presented in Figure 20.

Figure 20 shows that powder mixes with only small or large grains show the lowest inductance, whereas powder with original or bimodal distribution show the highest inductance. This means that the powders with a mix between large and small grains are favourable. Studies with coated powders were also performed. The coating is an oxide of 6–8 μm thickness. The thick coating affects the packing density heavily if all particles are coated.

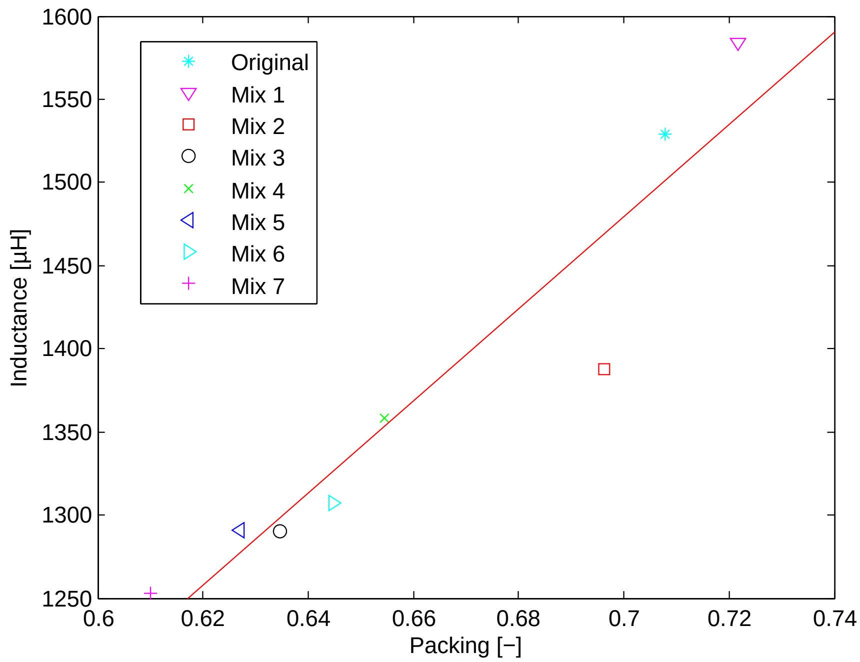

Figure 20: Measured inductance on tap density samples from Figure 19.

Therefore only the larger particles are coated, which affects the packing density less. Annealing can lower the losses in iron-silicon powders by reducing stress in the grain. Some of the powders were therefore annealed and compared with non-annealed powders. Powders that are used as delivered from the gas atomisation will hereafter be denoted as untreated powder. Powders that have been coated will be denoted as coated powder. Powders that have been annealed will be denoted as annealed powders. In Figure 21, a fracture surface of a typical SM^2C material is presented, showing the distribution of large and smaller particles. The particle packing is quite optimal in this case, about 70 % due to randomly packed particles. The wetting and isolation of particles is also apparent in the picture.

5.2 Manufacturing methods

The iron-silicon particles are in a state that prevents them from deforming plastically during forming and manufacturing of the soft magnetic part.

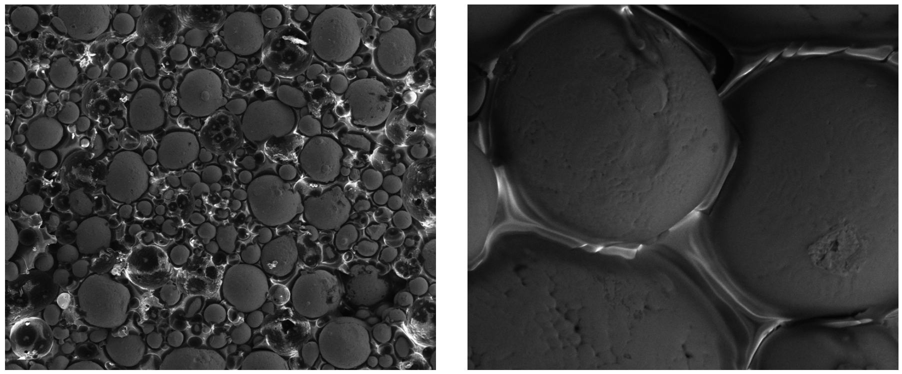

(a) 65x magnification.
(b) 800x magnification

Figure 21: SEM picture of a fractured SM^2C surface [18].

The manufacturing process must be optimised towards an ideal packing of spheres in a given space, leaving a minimum of remaining binder phase and, of course, a minimum of pores and air pockets. Several processing methods were investigated by the author, such as gravitational moulding, rotational moulding [50], vacuum moulding, and vibrational moulding. The research group at the Division of Production and Materials Engineering have earlier also tried injection moulding, but ruled it out due to low particle packing of the iron-silicon powder [51]. It is also possible to increase the properties by particle alignment in a magnetic field [52], but this has not been a part of this work.

The different manufacturing methods evaluated in this thesis are presented below with a short process description.

Gravitational moulding process:

1. The mould, powder and epoxy are preheated to the predefined temperature.
2. Powder and epoxy are carefully mixed by hand to minimize air bubbles and poured into the mould.
3. The mould is placed in the oven at the predefined temperature until it is cured.

Rotational moulding process:

1. The mould, powder and epoxy are preheated to the predefined temperature.

2. Powder and epoxy are carefully mixed by hand to minimize air bubbles and poured into the mould.
3. The mould is placed in a rotational device, exerting a centrifugal force of 26 G for 10 minutes.
4. The mould is placed in the oven at the predefined temperature until it is cured.

Vacuum moulding process:

1. The mould, powder and epoxy are preheated to the predefined temperature.
2. Powder and epoxy are carefully mixed by hand to minimize air bubbles and poured into the mould.
3. The mould is placed in a vacuum chamber at 0.1 bar for 15 minutes.
4. The mould is placed in the oven at the predefined temperature until it is cured.

Vibrational moulding process:

1. The mould, powder and epoxy are preheated to the predefined temperature.
2. Powder and epoxy are carefully mixed by hand to minimize air bubbles and poured into the mould.
3. The mould is placed in a vibrational device for 2 minutes with an amplitude of 0.2 mm.
4. The mould is placed in the oven at the predefined temperature until it is cured.

Using low viscosity epoxy resins is beneficial for the moulding process. After the SM^2C slurry has filled the form cavity, it is placed in an oven for curing at a determined temperature. After a specific time, demoulding takes place, either in a warm or cold state. Using the selected epoxy system, a post curing for four hours at 180 °C to reach its maximum glass transition temperature is necessary. This is performed after demoulding of the part.

The tests were performed on the same powder batch and three specimens were produced of each kind. In an initial test, simple rods were moulded in order to save material and time. The rods were used to investigate how the process temperature affected the packing of the material. The different treatments of the powders were also investigated at this stage (see Figures

22 and 23). The vibrational and rotational moulding processes show similar results up to 90 °C, but deviate from each other at higher temperatures. This is probably because the moulds were cooled during rotation. This means that the moulds must be actively heated during the rotation in order to achieve a higher particle packing at temperatures above 90 °C. The vacuum moulded process is better than the gravitational moulded process due to less air bubbles trapped in the material. It is seen that they have the same particle packing at 105 °C, which would indicate that the high temperature lowers the viscosity enough to let the air bubbles out without using vacuum.

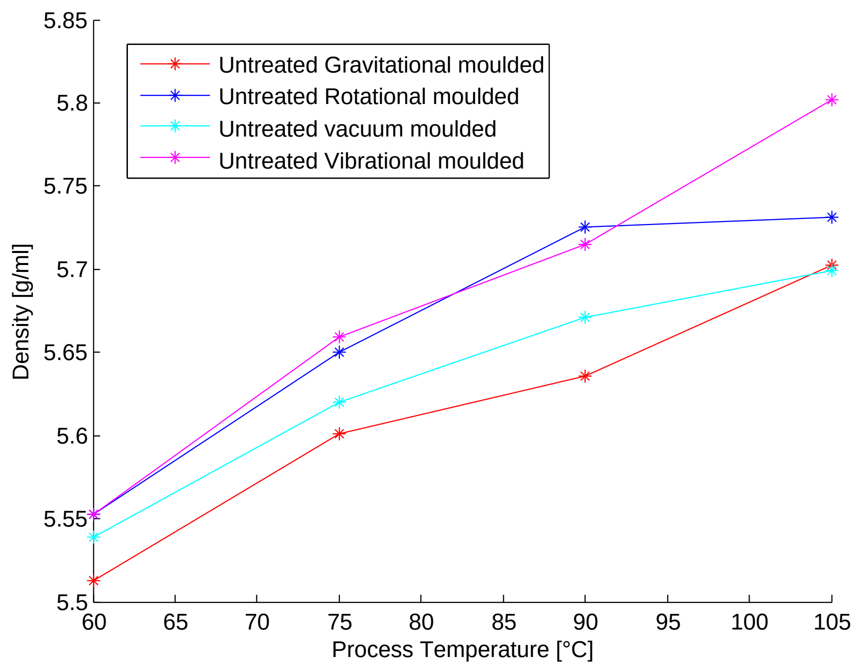

Figure 22: Comparison of manufacturing method as a function of process temperature.

The results in Figures 22 and 23 show that the particle packing will increase with increased temperature, for all except the rotational moulded samples. The processing temperature chosen for the continued experiments was 120 °C. The next step was to investigate how the permeability and losses of the materials were affected by the processing method. For these tests small cylinders 56 mm in diameter and 40 mm long were manufactured. Two of each variant were moulded and each cylinder was machined into two

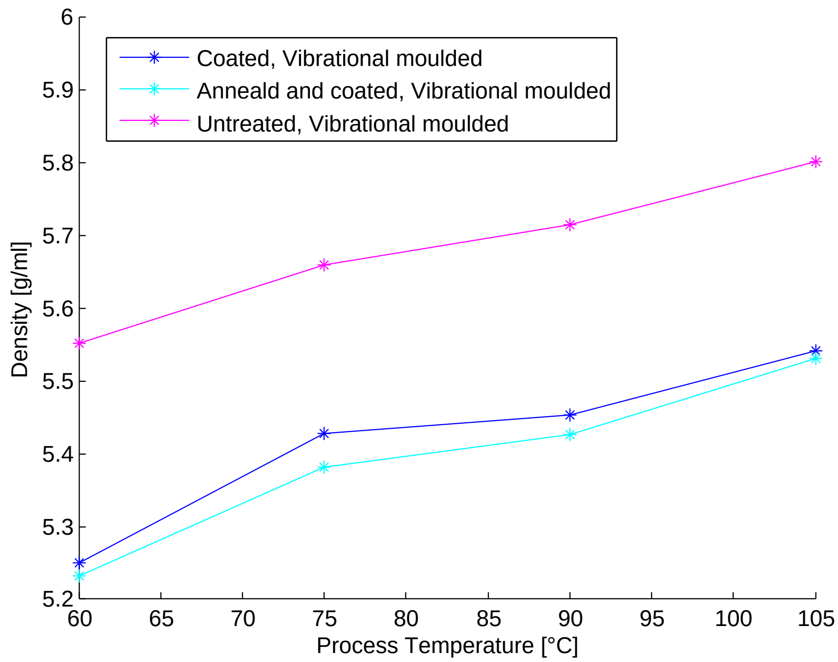

Figure 23: Comparison of how the process temperature and powder treatments affect the particle packing

toroids with the dimensions: 55 mm outer diameter, 45 mm inner diameter and 5 mm length. One of the benefits of the material is that it can be moulded into any shape, however small parts tend to get lower packing. A larger shape was therefore moulded and machined. A small cylinder, 20 mm diameter and 5 mm length, was machined. The smaller cylinder was used for measuring the dielectric strength.

In most cases, moulding to net shape is desirable, which is easy to achieve with SM^{2}C. But in some cases machining of the part is wanted or necessary. It is easy to machine a moulded part either in a milling machine or a turning lathe. The reason for this is that the matrix binder consists of epoxy, with relatively good machinability. The powder acts as a filler, keeping the epoxy matrix from cracking. Most other similar soft magnetic materials are harder to machine such as ferrites and SMCs. The relatively good machinability makes it possible to mould blocks and then machine the block to a desired shape. This makes SM^{2}C especially suitable for building prototypes.

The permeability and loss results can be seen in Figures 24 and 26. The particle packing is calculated from the density of the sample. Two trend lines are plotted in Figure 24, one for uncoated powder and one for coated powder. By using the trend lines it can be noted that the difference in particle packing for the same permeability is between 4 and 6 percent by volume.

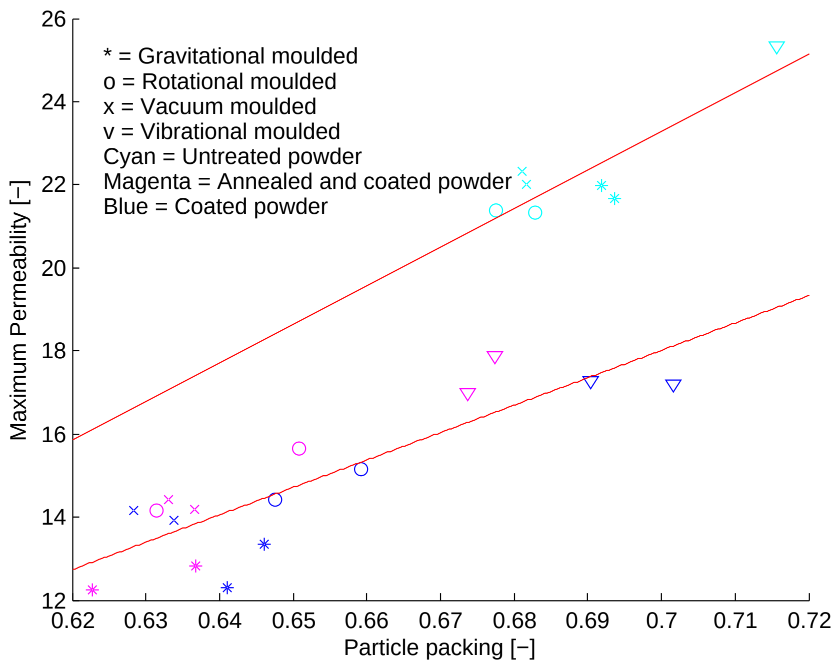

Figure 24: Comparison of different powder treatments and moulding processes.

This can be explained by the coating of particles. The coating is 6–8 μm thick, which on a 250 μm thick grain means adding 15 % of its volume without changing the permeability. This means that there are roughly 15 % of coating in the composite. Taking this into account, calculating the particle packing, both lines coincide quite well (see Figure 25). All particle packing calculations here after are compensated for the coating thickness.

Figure 26 shows a comparison of loss between different treatments. The annealed and coated powder shows a lower loss compared to the loss of the coated powder. The annealing lowers the losses by reducing residual stresses and increasing the grain size in the iron-silicon powder. The losses are higher

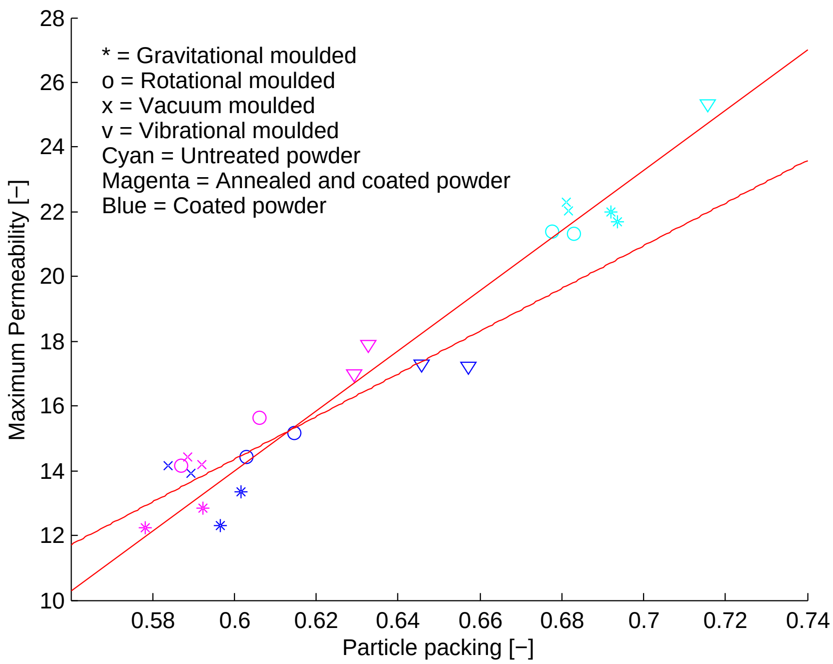

Figure 25: Comparison of different powder treatments and moulding processes, after compensation for coating thickness.

in the coated powder compared to the untreated powder. This is due to an oxidation in the surface of the iron-silicon grain during coating. The coating is not optimal with respect to magnetization losses, but there would be a dielectric breakdown for long-time usage in elevated temperatures for non-coated particles. The dielectric breakdown voltage on newly manufactured parts can be seen in Figure 27. The untreated samples show a dielectric breakdown below 2 000 V/m, most of them even lower, whereas most of the coated samples show a dielectric breakdown between 25 000 and 15 000 V/m. It is only the vibrational moulded samples that show a dielectric breakdown lower than 15 000 V/m. This is a result of the higher particle packing, but it is also possible that the coating is damaged, to some degree, as a result of the vibrations during the moulding.

It is possible to mould sensors, coils and other soft magnetic material units directly into the SM^2C structure[46]. This makes it possible to combine several materials and use them more efficiently. Moulding a sensor directly

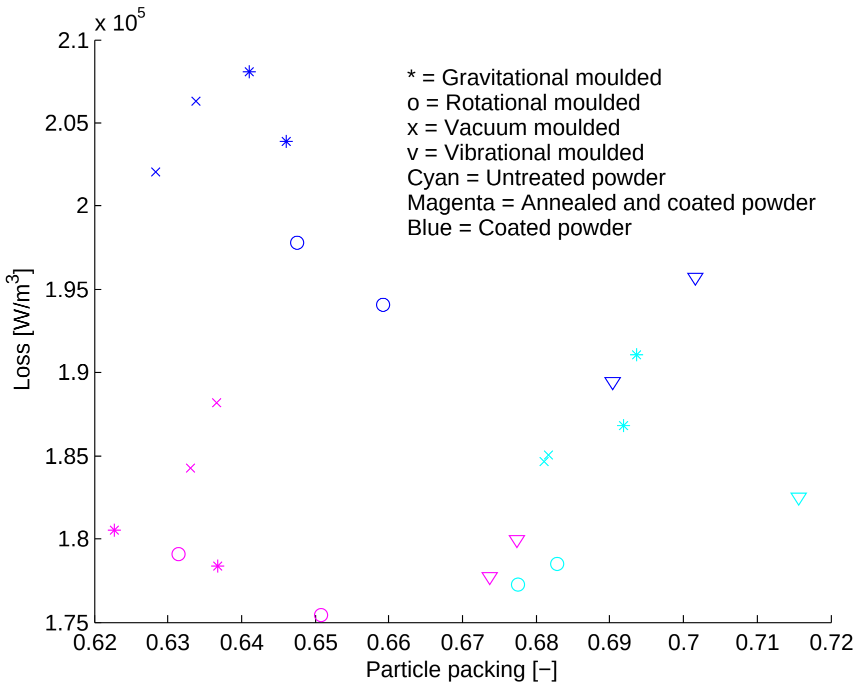

Figure 26: Comparison of SM^{2}C loss at 10 kHz and 0.1 T, with different powder treatments and moulding processes.

into the material may also shorten the production time and result in a superior product. One obvious disadvantage with this method is that it is sometimes difficult to accurately position the sensor or other part that is moulded inside the SM^{2}C. Therefore, it is necessary to design the product with this in mind.

In order to test the concept of combining functions, i.e. sensors, SM^{2}C, SMC and steel wire, a permanent magnet synchronous machine with four different stators was produced. The reason for testing on a motor is that it demands high geometrical accuracy when manufacturing, thus it will work well for evaluating the process.

The flux conductor in stator number one, Figure 28, consists of SM^{2}C moulded around pre-wound coils and sensors. The stator was rotationally moulded, with the centre of the rotation in the centre of the stator. The only manufacturing step after the de-moulding was to machine the outside to the right dimension.

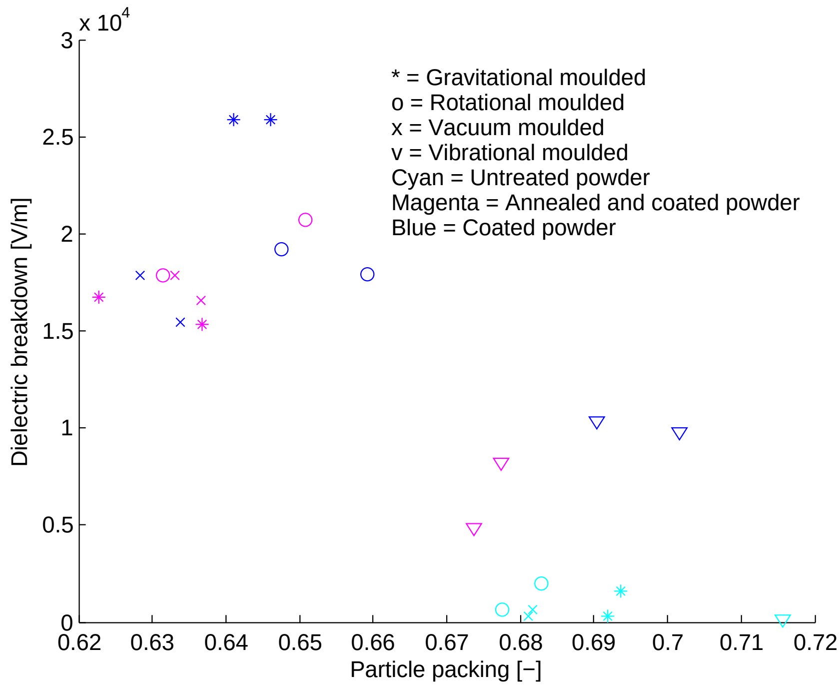

Figure 27: Dielectric breakdown comparison of different samples.

Stator number two, Figure 29, uses a winding wound around single SMC teeth, that were mounted in milled slots in the SM^2C backing. The voids around the teeth were filled with epoxy, and the outer diameter was turned to the right dimension.

Stator number three, Figure 30, uses the same materials as stator number two, but the winding consists of six segments instead of single teeth.

Stator number four, Figure 31, is produced in the same way as stator number three, but with a steel wire as backing instead of SM^2C in order to reduce the magnetic reluctance.

All four production approaches have their strengths and weaknesses. Stator number one is the easiest to manufacture, but the geometrical accuracy of the windings can be debated. The other stators involves more production steps but have a higher flux linkage. The superior, in this respect, is stator number four.

The problems with moulding the SM^2C around the sensors, coils and other soft magnetic materials is to position everything accurately. A choke or induction heater will be less affected by small errors in the positioning of the coil than the motor will have. However, there were no problems with combining different soft magnetic materials and sensors. The freedom to mould geometrically complex details as well as large and small parts are an advantage that most other SMC materials do not show. For more information see [46]

(a) Wound and moulded winding segment with sensors.

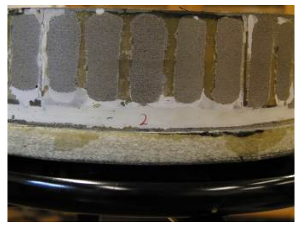

(b) Moulded stator that has been machined to the right diameter.

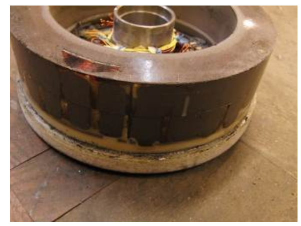

(c) Finished stator from top view.

Figure 28: Production phases for SM^{2}C moulded stator, Stator number one [46].

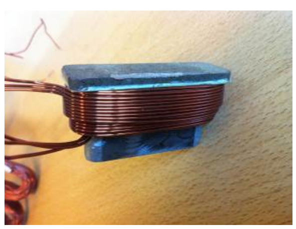

(a) Single tooth with winding and tooth tip.

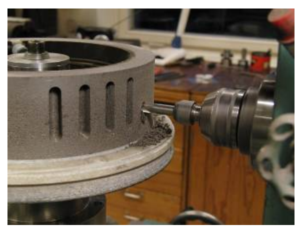

(b) Milling of slots in SM^{2}C backing.

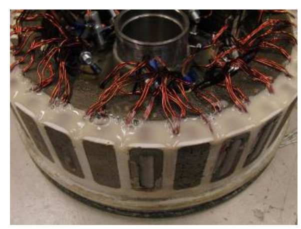

(c) Finished stator after turning.

Figure 29: Production phases of single SMC tooth wound stator with SM^{2}C moulded backing, Stator number two [46].

5.3 Soft magnetic mouldable composite properties

It is difficult to set a fixed value on any property for SM^{2}C because the properties varies depending on manufacturing process, temperature and powder batch, as can be seen in Figures 25 and 26. Multiple properties are shown for the material since it is possible to customise the properties within wide limits. Two different materials are presented; Firstly, the one with the highest permeability, which is vibrational moulded, untreated powder, and secondly,

(a) Winding.
(b) Stator during mounting of winding and teeth.
(c) Finished stator.

Figure 30: Production phases of SMC tooth wound stator with SM^2C moulded backing, Stator number three [46].

(a) Wound stator backing of iron wire after milling of teeth holes.
(b) Stator during mounting of winding and teeth.
(c) Finished stator.

Figure 31: Production phases of SMC tooth wound stator with iron wire wound stator backing, Stator number four [46].

the one with the lowest permeability and the highest loss, in other words gravitational moulded, coated powder. The results in Figure 32 show that the frequency of the applied field does not significantly affect the relative permeability on the material. However, the relative permeability is reduced with increased magnetic flux density for the sample with high relative permeability. The sample with lower relative permeability shows a more modest reduction of relative permeability with increased magnetic flux density. This is because the demagnetising field, seen from an individual particle in a composite with a higher particle packing, will be reduced, thus saturates at lower flux density. The losses in the material versus flux density on the x-axis, Figure 33, can almost be considered as straight lines in a log-log diagram, as expected. It can be noted that the difference in loss between the two materials is small regardless of the considerable difference in permeability.

The fitting coefficients from the Steinmetz equation, Equation 6, are

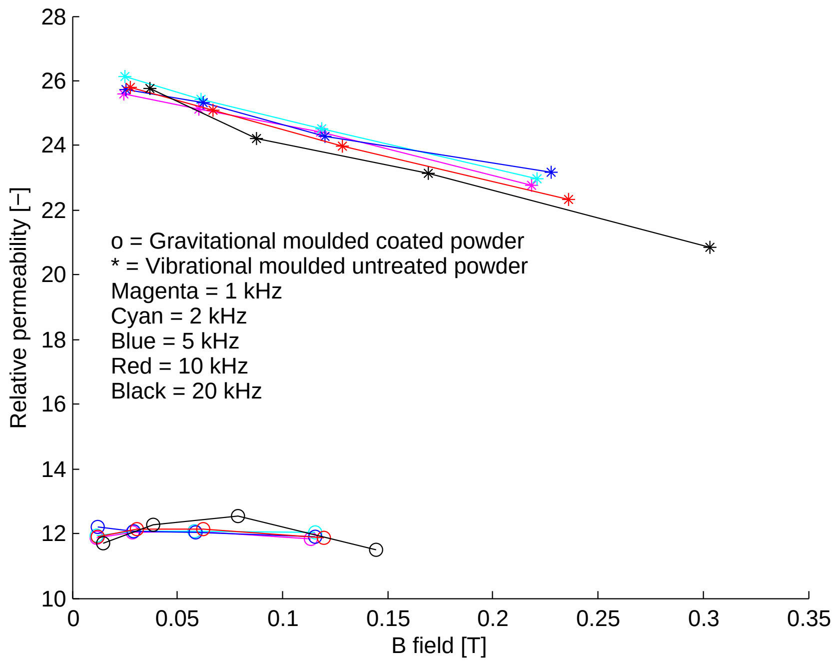

Figure 32: Permeability as a function of B field at different frequencies for a vibrational moulded sample using untreated powder and a gravitational moulded sample with coated powder.

derived from the measured samples and are presented in Table 1. The α coefficients are almost identical, which means that the loss due to frequency is, more or less, the same. The β coefficient is lower for the untreated sample, which means that it is less affected by the magnetic flux density than the coated sample.

Table 1: Steinmetz coefficients derived from the measured samples.

Powder treatment	**Processing method**	k	α	β
Coated	Gravity moulded	212	1.22	1.90
Untreated	Vibrational moulded	133	1.23	1.77

The properties in Table 2 should be seen as indicative values for the SM^2C material, since the different manufacturing processes will give slightly different properties.

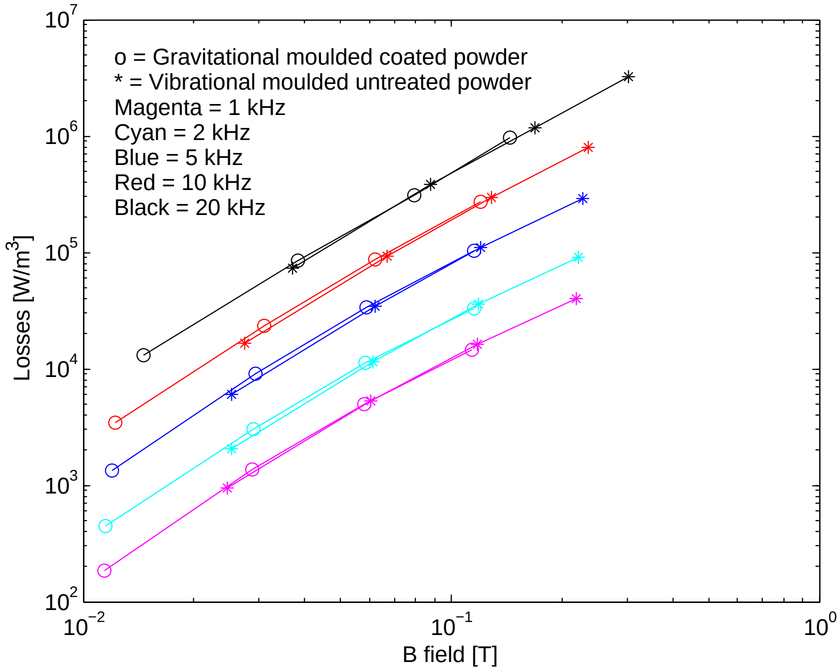

Figure 33: Loss as a function of B field at different frequencies for a vibrational moulded sample using untreated powder and a gravitational moulded sample with coated powder.

Table 2: Representative values of some measured data for SM^{2}C.

Bending strength	130 MPa
Thermal conductivity	2.2 W/mK
Saturation magnetisation	1.3 T @ 150 kA/m

6 Winding design for SM^2C applications

The coil geometry or winding arrangement is the single most important component in many electromagnetic applications. The winding design is the key to generate a sufficient electromagnetic field without getting overheated. Traditionally, the components are built around a yoke, and the winding work is one of the final activities in the production process. The SM^2C material gives an opportunity to design windings in a totally new way due to the moulding capabilities. Instead of starting with a machined yoke, the technology allows production of optimised winding designs as the first manufacturing activity. By preparing the winding before the moulding process and placing the winding in its correct position, an increased geometrical freedom and a higher fill factor can be achieved than for traditional windings.

6.1 Design

Commercial products have often gone through a number of iterative improvements to find a good tradeoff between cost and performance, based on the selection of materials, design and manufacturing methods. To develop a significantly better product, not only one of these factors is enough to change, but they are linked together. While the SM^2C material provides new manufacturing opportunities, the design need to be adjusted not only to reflect alternative production methods, but also due to the change of material properties. Considering electric motors for example, soft magnetic composites have lower permeability than traditional laminates, which makes it necessary to adjust the geometry in order to shorten the magnetic flux paths. Also magnetic saturation occurs at lower level, to the advantage of reduced losses at high frequencies, promoting high speed, multi-pole motor types. By utilizing the three-dimensional material properties in the best possible way, the benefits of the material can be employed, while the effect of the drawbacks can be displaced.

The actual design of the winding of course depends on the electromagnetic application, but from a generic perspective, a motor, choke and induction heater feature similar production challenges. New soft magnetic materials still allow the windings to be produced in the same traditional way, but to really make the most of the SM^2C material, moulding of the core material around the winding is preferred. If the winding is to be moulded inside, a preformed stable winding is crucial. It is also necessary to be able to position the winding securely in the mould. The winding stability and positioning means that design for manufacturing is important, as it enables the utilisation of the materials' manufacturing benefits of moulding. In this work, both traditional manufacturing methods and more innovative approaches have been tested in order to evaluate the differences. Designs that have been investigated include: transversal flux [41, 43], wave windings[44, 53, 45, 54] and different variants of distributed concentrated windings[44, 9, 45] (see Figure 34). There have been both single phase and three-phase motors.

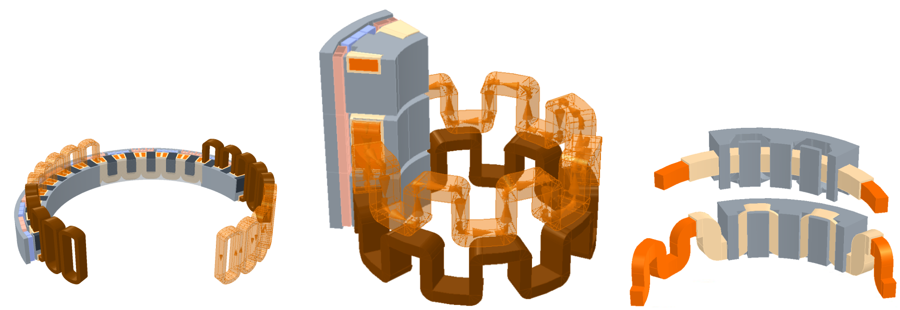

(a) Distributed concentrated winding.

(b) 3-phase wave winding.

(c) Transversal flux winding (on top) that can be reshaped to a wave winding (bottom).

Figure 34: Different coil designs used for motor prototypes.

The designs for the induction heating windings and the choke coils are usually simpler than the motor windings. Some designs that have been tested for choke applications are a type of coil wound like an axially compressed solenoid coil with different geometries and turns (see Figure 35a). The chokes have been designed and manufactured in different sizes, from 60 mm in diameter to 200 mm in diameter. The induction heater windings are sometimes wound like a solenoid or axial flux coil, and sometimes a flat spiral or face coil (see Figure 2a) [37, 38, 8]. Typical size ranges from 300 mm to 1500 mm in length. Mainly litz wire has been used in the windings to reach a high efficiency due to the frequency applied in the chokes and induction heating applications.

6.2 Manufacturing

The manufacturing of windings can be one of the most challenging tasks in the production of electromagnetic components. That is because sufficient electrical insulation must be ensured as well as good geometrical stability

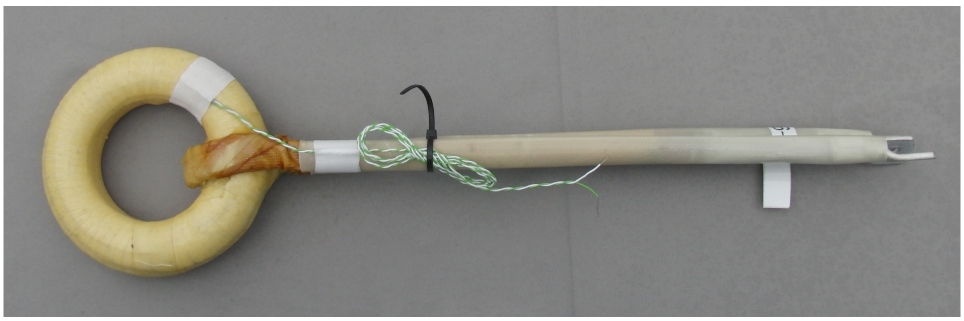

(a) Choke coil with temperature sensor.

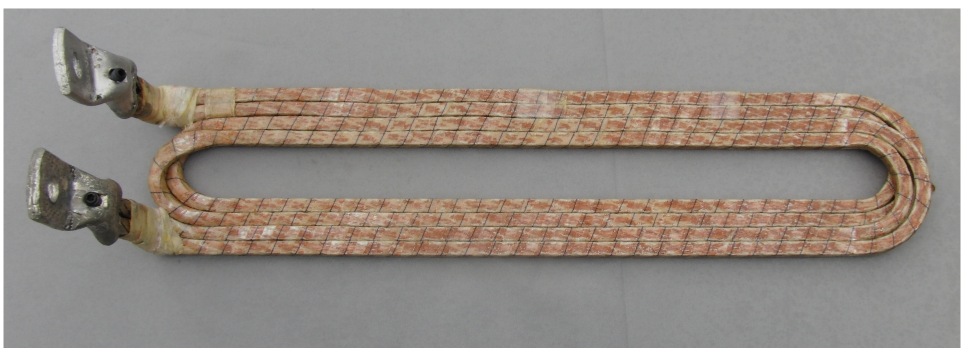

(b) Induction heater coil with two turns.

Figure 35: Two different coil designs.

and high fill factor, still within a limited production cost. Electrical insulation is the most important property, since a short circuit will damage the device and affect the safety of the entire system. For example, for induction heaters and chokes there are generally larger margins regarding the geometrical accuracy, still affecting the performance. By maximizing the fill factor of the winding, the highest operational power will be achieved, which might allow to shrink the design with maintained performance without risk for overheating. The manufacturing of a winding is in many cases time consuming due to complicated design and small batch sizes. Most of the windings used in this thesis are wound by hand due to the small batch sizes and low number of turns.

When making prototypes or small batches, manual winding often applies, for large volumes on the other hand, automation is necessary. Depending on the application, there might be a trade off between manufacturability and performance. Using the results of this work, this can to some extent be overcome. In [55], a method was developed for manufacturing of high fill factor wave windings with high geometrically accuracy for electrical machines, allowing for a fully automatic production.

The wave winding is produced by a two-step method; first winding of a hoop coil and secondly pressing the coil to its final shape. A prototype of the wave winding can be seen in Figure 36. The dies used to press the winding will move axially and radially when forces are applied on them, and thereby create a wave winding, see Figure 37. The whole machine used to produce the prototypes can be seen in Figure 38.

The isolation of the wire will always risk getting damaged during manufacturing, and it may dramatically reduce the lifetime of the finished product. It is important to have this in mind when designing the manufacturing steps, as this is something that must be considered through the whole manufacturing process so that the winding will not get damaged during motor assembly, for example.

Windings are usually produced in one or two steps, where two is the most common method for motors, starting by winding of a loosely packed coil, which in turn is forced into the core. The second step is usually performed by machines for smaller motors and by humans for bigger motors. A rubber mallet or similar is often used when humans place the winding in the motor. In single tooth wound motors, the winding consists of one step only, but instead a complex assembly step is required. The most common for chokes are single step windings, automatically produced as solenoids or by a toroid winding machine. Industrial induction heaters generally consist of copper tube coils or hollow constructions produced by machining in combination

Figure 36: Wave winding with 35 mm press height [55].

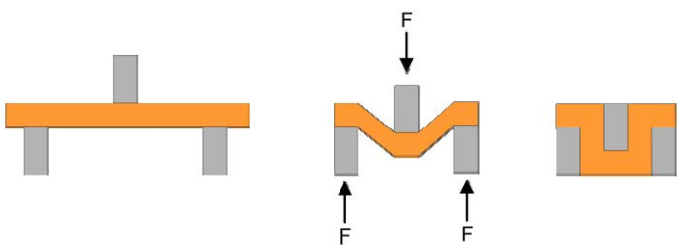

Figure 37: Principle of winding forming process, illustrated as 3 interacting dies(grey) forming part of a winding (orange) [55].

with brazing and recently also by additive manufacturing [56]. Using litz wire based induction coils, automatic winding machines can be used in the production.

Different winding methods were used in this thesis. Stator one, Figure 28b, was manufactured by winding the wire in a mould and infiltrate it with epoxy. Stator two, Figure 29a, was manufactured in a single step by a winding machine directly on the tooth. Stator three and four, Figure 30a, were manufactured by winding the wires in a mould, but without infiltrating before mounting on the stator. The induction heater coil in Figure 35b was produced by winding the litz wire in a mould and infiltrate it with epoxy to get stability. The choke coil in Figure 35a was wound in a machine and

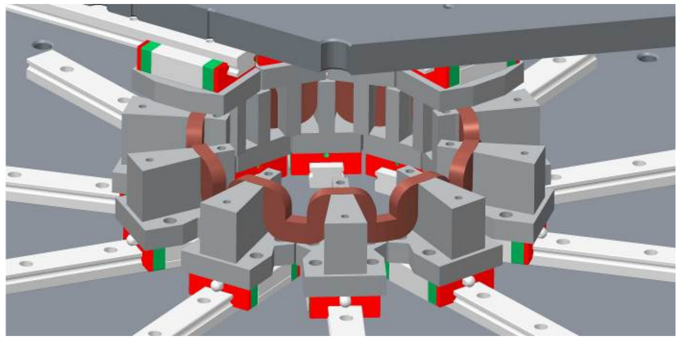

Figure 38: CAD-model of the winding forming machine with pneumatic cylinders [55].

then taped with nomex to achieve stability and isolation.

Design for manufacturing is very important with the wide range of designs that is possible. The wave winding presented in [55] show that a proper design for manufacturing can be found in order to take advantage of the SM^{2}C concept.

6.3 Thermal conductivity of windings

The limiting factor when designing magnetic components is the heat buildup in the device. Two main heating sources can be identified, losses in the soft magnetic material and in the winding, where the latter often is the dominant one. For certain applications, for example induction heating, also external heat sources must be considered in the thermal design. Therefore, it is important to have accurate data of the thermal properties of all different materials, including the windings, [57, 58, 59, 17].

A typical winding consists of a stack of enameled copper wires, with severe anisotropic properties. Not only the varnish affects the thermal properties, but entrapped air is devastating for the thermal conductivity in the lateral direction. Traditionally it has been difficult to measure the thermal conductivity in the lateral direction of a non-infiltrated winding since a cutout will cause the strands to fall apart. By using a Hot Disk 2500S [33] thermal testing machine, both isotropic and anisotropic samples can be analyzed. The latter can only be done if the sample is isotropic in the plane of the measuring sensor, which a winding is. By clamping the wires together before cutting, a winding could therefore be measured on before and after infiltration in order to get a proper comparison. The results are then compared in [16] with finite element analysis (FEA) and the Hashin and Shtrikman approximation [60, 61, 62].

The results of an infiltrated winding can be seen in Figure 39. It shows a good agreement between measured values, FEA and the Hashin and Shtrikman approximation.

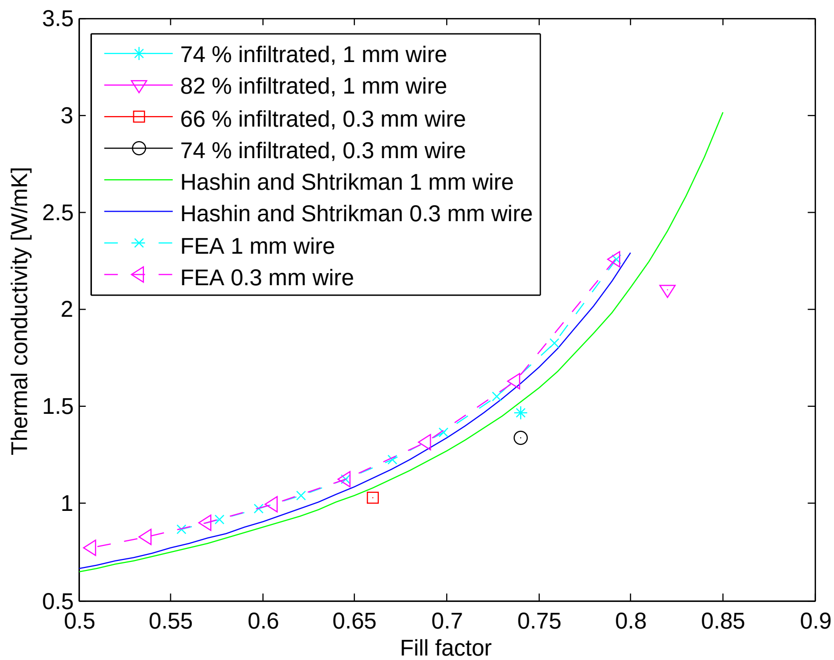

Figure 39: Comparison of the Hashin and Shtrikman model with measured data from infiltrated samples [16].

Results from the non-infiltrated windings can be seen in Figure 40. The Hashin and Shtrikman approximation shows a reasonable agreement with the measured values, but the FEA are not in a good agreement. This is because the FEA is assuming that the coating on the wires are not deformed or touching each other. In reality the coating is deformed and therefore an increased thermal conductivity is obtained.

It can be concluded that there is a big difference between the thermal conductivity in the infiltrated versus non-infiltrated winding. This is important to know when designing a motor, induction heater or a choke in order to get the best efficiency, using a proper production method, and to achieve the desired design to the right price.

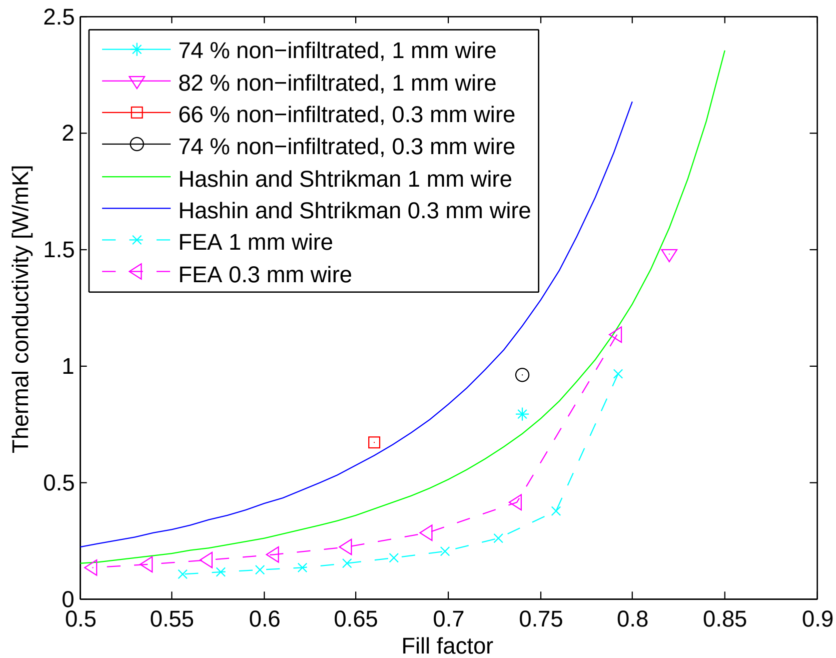

Figure 40: Comparison of Hashin and Shtrikman with measured data from non-infiltrated samples [16].

6.4 Insulation of winding

The insulation on electrical conductors are critical in order to avoid short circuits and potentially dangerous machines. A thin, evenly distributed insulation with high thermal conductivity is desired in order to dissipate heat from the electrical conductor to the SM^{2}C material. The better cooling capability, the higher current density can be used and thereby more output power is obtained. An example of a winding moulded inside SM^{2}C without any extra insulation, except for the thin varnish layer on the wire, is seen in Figure 41. Many conventional insulations for motors and other electromagnetic devices involves winding a paper like tape around the coil. This however traps air and thus lowers the thermal conductivity. An insulation that is applied by dipping or spraying directly on the winding is therefore desired.

Figure 41 illustrates one of the benefits of the SM^{2}C material, and also one of the challenges. Some of the iron powder particles are only a few μm

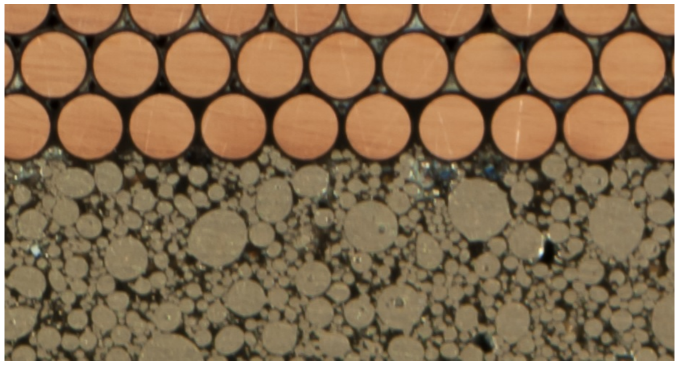

Figure 41: Picture of the winding and the core material. The wire is 0.5 mm in diameter.

in diameter, and can thereby penetrate small pinholes in the insulation. A study in [11] reveals that a single layer of the tested coatings was not enough to pass the test requirements. Several layers were needed to be applied for all coatings tested. The reason is that pinholes are practically unavoidable and difficult to cover by extra coating layers, given that methods applicable for implementation in large volume manufacturing processes are used. The tested coatings are shown in Table 3. Not all of them fulfilled the criterias, but are included in order to provide an adequate overview of available coating systems and to show their electrical performance.

Table 3: Overview of the coatings used.

Material	**Manufacturing process**
Ultimeg 200/380	Dipped and baked at elevated temperature
Voltatex 4250	Dipped and baked in UV-light
INFRALIT PE 8350	Powder coated and baked at elevated temperature
Epoxy MagComp	Dipped and baked at elevated temperature
MF 8001 NV	Baked while saturated in resin
Parylene N	Chemical vapour deposition

The coils (Figure 42) were coated with different numbers of layers, in accordance with each manufacturer's recommendations, and then tested as described in section 4.4.

The coil should be able to withstand 3 kV DC for 1 minute in order to pass the test. It can be concluded that none of the coils passed with only one coating layer. See [11] for full results.

Figure 42: Uncoated coil [11].

More tests were performed with up to five layers of coating in order to investigate the necessary thickness to pass the test. The only one that passed was INFRALIT PE 8350, with only two layers. The reason for this is that the thickness of the INFRALIT PE 8350 coating is rather thick compared to the other coatings (see Figure 44).

It can be noted that on some of the coils the coating was uneven. This was especially noticeable on the ones with a large number of coatings. The Ultimeg 2000/380 was chosen for coating new coils that were cured while rotating, which could result in a more even coating. The results can be seen in Figure 43, and show that the rotation increased the dielectric strength of the coil coating. Three layers are still not enough, but with six layers a dielectric strength of minimum 3500 V can be achieved. The coils with 9 and 12 coatings held for the maximum output voltage that the test equipment could deliver of 5 kV.

A cross section of a coil coated with INFRALIT PE 8350 and coils coated while rotating with Ultimeg 2000/380 can be seen in Figure 44. It can be seen that three layers of Ultimeg 2000/380 does not significantly affect the geometry of the cross section. Six layers start to affect the geometry to some degree, and nine layers affect the geometry significantly. This is important to know when designing the machine in order to use the right tolerances and measurements. The INFRALIT PE 8350 with two layers shows a similar effect on the cross sectional geometry as the Ultimeg 2000/380 with six

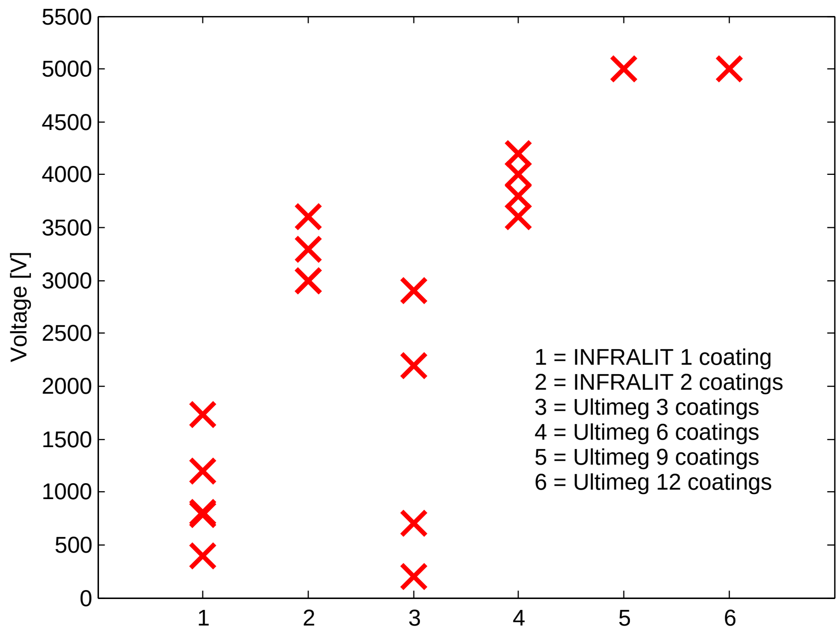

Figure 43: Coils coated with INFRALIT or PE8350.

layers. They also have a similar dielectric test result, which means that either of the two coatings could be used when coating a coil.

The thermal coupling between the SM^2C and the coil will be negatively affected by the coating; therefore, the thickness should be minimised. However, this type of coating is preferred compared to more traditional isolations such as tape or film, where trapped air will lower the thermal coupling even more.

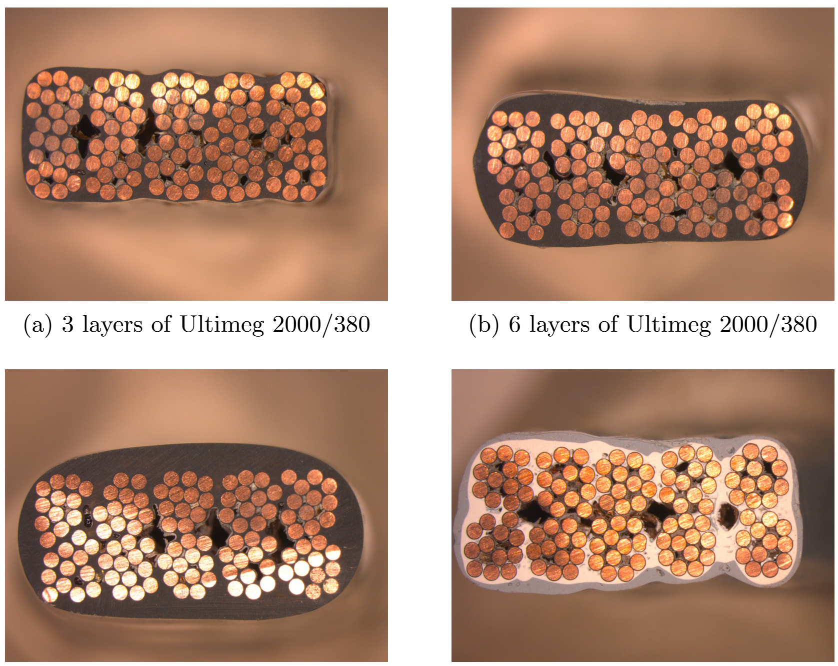

(a) 3 layers of Ultimeg 2000/380

(b) 6 layers of Ultimeg 2000/380

(c) 9 layers of Ultimeg 2000/380

(d) 2 layers of INFRALIT PE 8350

Figure 44: Cross section of coils coated with different number of layers and coatings [11].

7 Electromagnetic and thermal multiphysics simulation

Simulation in some form is necessary to design an efficient new motor, choke or induction heater. In order to perform a simulation, data of the component materials used in the model are required. Electromagnetic modelling is the most elemental type of simulation due to the nature of the inductor; however, the limitation of an inductor is often temperature. This means that the temperature of the inductor also should be simulated. Thus, a multiphysics simulation with coupled magnetism and heat transfer is chosen. In order to verify the simulation model, it will be compared with measurements on a prototype induction heater. This section focuses on one particular inductor geometry for induction heating applications. The geometry of the induction heater is chosen because it can be simulated using a two-dimensional axisymmetric model.

Simulations and measurements on an induction heater has been performed in order to test the method and the collected data [32]. The procedure is described below and can be implemented for both chokes and motors. The knowledge from the simulation can be used to understand which properties of the different materials should be focused on in material development. The model can also serve as a useful tool for optimising inductor properties.

7.1 Simulation model

The simulation tool chosen is Finite Element Method Magnetics (FEMM) due to the possibility to calculate losses caused by skin and proximity effects in litz wire and to employ non linear B-H relationship losses in the soft magnetic material [63, 64, 65, 66, 67]. Matlab is used in order to transfer data on element level from the magnetic simulation to the heat simulation. This is performed through a Matlab script in order to communicate with the FEM program through the built in OctaveFEMM interface, that collects data in one simulation and transfers them to the next. This is iterated until the total loss increase is less than 0.1 W.

Two different models are used in order to evaluate every important parameter. The initial setup is without any workpiece (see Figure 45). It is cooled at the bottom at an even temperature and insulated at the sides and at the top. It is run with both AC and DC currents in order to investigate the different properties. At a first step, DC is used to calculate the thermal conductivity of the litz wire, without any losses in the soft magnetic composite material and only the resistive losses in the wire. At a second step, AC is used to calculate the iron losses created in the soft magnetic material.

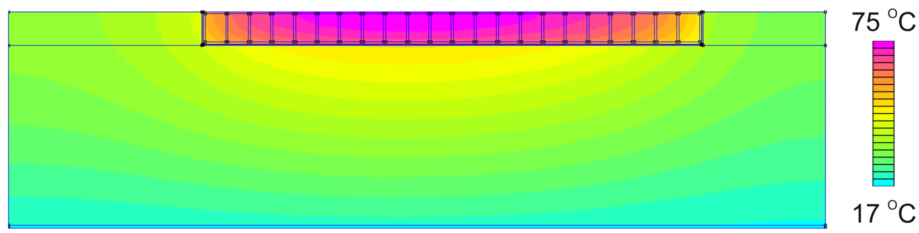

Figure 45: Heat simulation of the inductor without a workpiece on DC [32].

The second setup has an aluminium workpiece and uses a frequency range of 15–25 kHz. Figure 46 also show the "resolution" of the power loss transferred from magnetic simulation to thermal simulation. For further details see [32].

Both models are run at different powers and the AC is run at different frequencies.

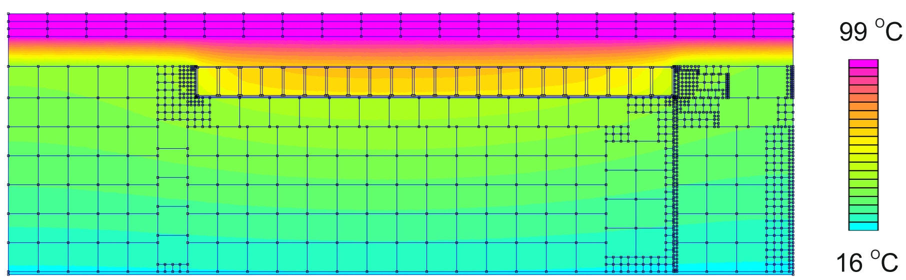

Figure 46: Heat simulation of the inductor with a workpiece at 20 kHz [32].

7.2 Test setup

The inductor is insulated with 90 mm thick insulation on the sides and at the top when run without load, Figure 47. The insulation is only applied on the sides when a workpiece is used, Figure 48. The bottom is cooled with an aluminium cooling plate that is kept at a fixed temperature. At the first step only DC is used in order to only generate resistive losses in the litz wire. The temperature is measured with thermocouples moulded inside the SM^2C. The collected data can then be used to compare with simulated values from FEMM, see [32] for further information.

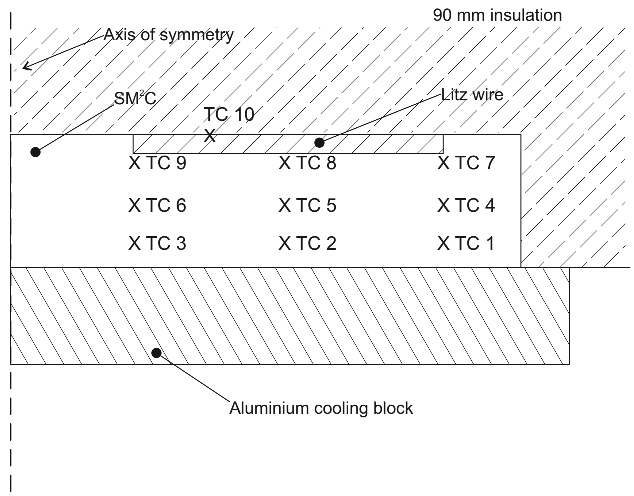

Figure 47: Thermocouple placement on a schematic test setup 1 without load [32].

The second step is to run the same setup as before with AC instead of DC. By running it with AC the iron losses in the SMC material can be calculated.

The third step is to run the same setup with AC and a load, in this case an aluminium pot filled with boiling water on top of the heater (see Figure 48). A load is used because this is the most common way to use an induction heater, and where the accuracy of the model is most important. A workpiece is also necessary to be able to verify the magnetic properties of the SMC material.

7.3 Results

When comparing the simulated results with the experimental results for the DC case, a good agreement can be seen. The steady state temperature difference results can be seen in Table 4, and the results for the 50 A test are illustrated in Figure 49.

When looking at sensor TC 10 in Table 4 it can be noted that the first/lowest four currents show good agreement between simulation and measurement. The last/highest current however show a relatively poor agreement. This is thought to be explained by the increase of the temperature, since only the properties in the litz wire are compensated by temperature. However, there is good agreement between the simulated and the experi-

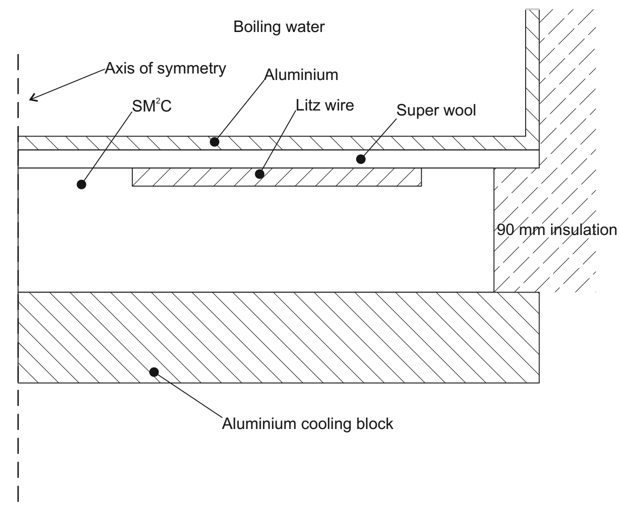

Figure 48: Schematic of test setup 2 with aluminium load [32].

mental results for the other nine sensors in all measurements. Therefore, the simulation model is seen as a good representation of the experimental setup at temperatures up to 70 °C with DC current excitation.

A comparison of the losses in the litz wire show that the simulation is underestimating the values compared to the measured ones. This is a problem since the thermal generation in the litz wire is the largest contributing heat source. This is solved by measuring and simulating the losses on a naked coil and then compensating with a factor for each current. This is however not a perfect compensation due to proximity effects.

A sensitivity analysis was performed in order to identify the impact from different material parameters. The parameters were changed by ± 10 % from their nominal value. The results can be seen in Figure 50, and to be noted is that the copper resistivity together with the thermal conductivity are the most influential parameters. The copper resistivity is hard to change, but a larger cross section could be a solution if their is enough space for the application. The thermal conductivity could be increased by adding a filler with high thermal conductivity, without decreasing the particle packing. Another solution could be to increase the particle packing, and thereby increasing the permeability of the soft magnetic material.

Table 4: Temperature deviation in °C between simulated and measured values. From largest to smallest deviation; red, orange, dark green, light green. The numbering of the thermocouples correlate with the numbering in Figure 47 [32].

	40 A	**45 A**	**50 A**	**55 A**	**60 A**
TC 1	1.99	1.73	1.41	0.55	-0.09
TC 2	2.16	1.81	1.71	0.99	0.11
TC 3	-0.14	-0.90	-1.50	-2.73	-4.16
TC 4	2.40	2.59	2.82	2.46	1.95
TC 5	1.31	1.12	1.13	0.10	-1.66
TC 6	2.26	2.18	2.14	1.51	0.63
TC 7	-3.04	-3.45	-4.00	4.62	-5.53
TC 8	0.65	0.84	0.50	-0.17	-1.06
TC 9	1.46	1.31	1.12	0.18	-1.12
TC 10	0.92	-0.35	0.48	-1.72	-6.55

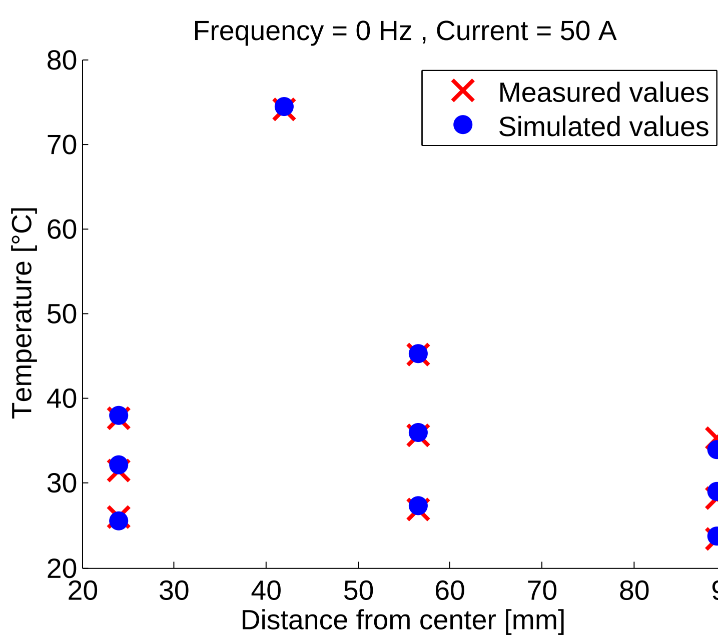

Figure 49: Comparison between simulated and measured temperatures at 50 A DC [32].

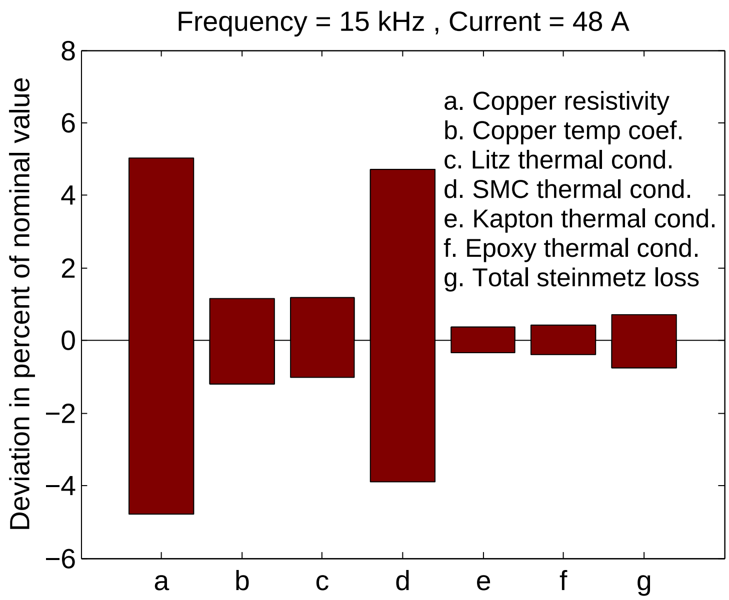

Figure 50: Sensitivity analysis of seven key parameters in the simulation model, performed without load and compensation of losses. The temperature from the simulation used is the one on top of the litz wire, TC 10. The y-axis is calculated by dividing the temperature deviation from nominal value by the nominal value in °C [32].

8 Application cases

The SM^2C material has been evaluated in several projects and prototypes. A selection of them are presented here in order to demonstrate the potential of the material and how well it works in different applications together with the coil and sensors. Not only typical academic research projects are included, but also some industrial spin-off applications are briefly presented.

8.1 Electrical machines

Several concept electrical motors have been designed and produced in different projects, but the author's main focus has been the in-wheel motor concept.

8.1.1 In-wheel motors

In-wheel motors can be used in many types of vehicles, in the project DAMIA2 they were intended for vehicles for disabled persons. The studied design was a three-wheeled motorcycle where the two rear wheels would contain in-wheel motors (see Figure 51 and 52). The intention was that a person in a wheelchair should be able to run the wheelchair onto the motorcycle, attach it in a simple manner, and then drive the vehicle in a normal way.

Figure 51: Early mockup of three-wheeled motorcycle.

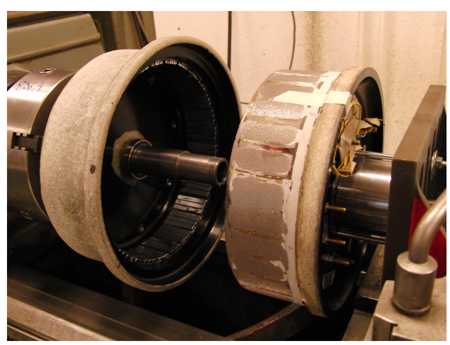

Figure 52: Mounting of stator 1 in to the rotor.

In the project, four different in-wheel motors were built in order to evaluate the production of the motor and also the performance of the finished motor prototypes. All of the four motors had the same rotor and the same stator geometry. Coil configurations and soft magnetic materials combinations were changed between the different motors in order to evaluate the different material compositions and manufacturing methods. A more extensive explanation of the different setups can be found in section 5.2.

The evaluation of the motors showed that employing a pure SM^2C core would result in low torque. Using 5P Somaloy 700 HR inserts increased the flux linkage, but it was still significantly lower than if a pure 5P Somaloy 700 HR setup was to be used.

8.2 Induction heating

8.2.1 GreenHeat

A lubrication oil is usually applied when sheet metals are deep drawn in order to reduce the friction coefficient. The oil must be removed before painting, and this is usually performed either by washing away or evaporating the oil. For the oil to evaporate it needs to be heated to at least 120 °C. The task for the project, called GreenHeat, was to develop a replacement for the 3 meter IR oven used in the present production line, which needed one hour of start-up time, with a more efficient heating unit. In the project an induction heating unit was developed as an alternative solution. The induction heating unit was only 1.2 meter by 0.8 meter, Figure 54 and had a start-up time of a couple of seconds. Power was only consumed when the metal sheets were heated by the induction coils. This meant that the heating unit did not consume any power during idling time, breaks or short stops. The six induction heating coils, Figure 53, were placed under the conveyor belt.

The induction heater was constructed from litz wire and the SM^2C material was moulded directly onto the litz coil . The SM^2C material was also moulded with integrated flanges in a way that it could be effectively air cooled by a radial fan on the backside of the unit. The GreenHeat concept has later been more carefully analysed and developed, and the results from this study is presented in [10]

The induction heating system was also tested in an industrial production environment for half a year with good results.

8.2.2 RaUCH

Cycling the temperature of a tool is necessary in many manufacturing operations, but this is often very time consuming and affects the overall productivity of the process. Long heating times are the consequence of employing tools with large masses, and the reason for this is to reach an even temperature over the whole tool surface, and to ensure a good quality of the produced item. Traditional heating in these systems is performed by heated

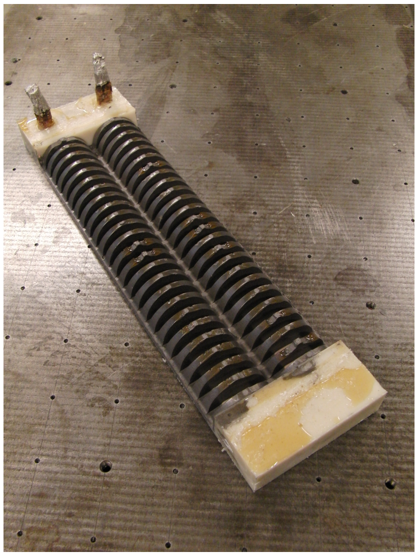

Figure 53: 1 of 6 induction heater coils used in the GreenHeat unit.

Figure 54: Complete GreenHeat oven during an exhibition.

oil or by resistive heat cartridges. A faster way of heating and cooling tool surfaces was developed in the RaUCH project. Induction heating of thin tool structures were combined with cooling by the use of liquid carbon dioxide. However, it is a challenge to achieve uniform temperature over a given surface using induction heating, due to edge effects etc. This was solved by introducing several induction coils working together in a travelling wave pattern. This approach will also give uneven heating at a certain point in time, but because the field is moving over the surface at a high speed, an even temperature will occur in a relatively short time.

The technology was implemented with two coils controlled by two power inverters. The coils can be seen in Figure 55a. The shape of the coil was designed to make it easy to simulate in a two-dimensional finite element method programme, as well as making it easier to interpret the measured data.

Laboratory tests showed that there were obvious coupling effects between the two coils, which demanded some type of compensation strategy. The results after compensation for both simulation and measurement can be seen in Figures 55c and 55d. The temperature pattern was not ideally even, but is was a great improvement compared to conventional heating and cycle times were brought down dramatically compared to conventional thermal cycling.

(a) Two-phase travelling wave inductor.

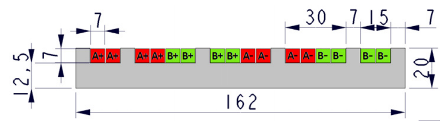

(b) Cross section of inductor with dimensions.

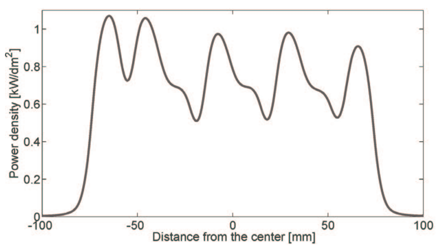

(c) Simulated power density across the wires of the two-phase inductor [38].

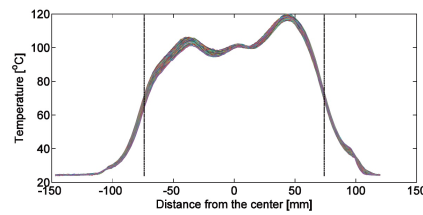

(d) Temperature profile of 200 different cross sections of the workpiece, distributed along the heated area [38].

Figure 55: Some results from the RaUCH project

8.2.3 InRoll

Mass production of food often involves many manufacturing like processing steps. Some foods are pressed or rolled, others are extruded. Kebab meat sold frozen in the supermarkets or to small restaurants is first extruded to round strings and then flattened with a roller before grilling. The meat is extruded at around 0 °C and will stick to the roller if the surface is not heated to at least 130 °C.

Heating the roller from the inside is the most practical approach due to the high hygiene demands. An induction heater was therefore designed and placed inside a stainless steel tube in the InRoll project [68]. The internal induction heating made it possible to minimize the start-up time as well as the the shutdown time, and also make it easier to clean the equipment. The temperature profile along the roll was a critical issue, and especially ends of the roll were carefully studied.

A transversal flux heater similar to the one in the GreenHeat project was initially evaluated in a smaller laboratory setup, but it turned out to be difficult to get an homogeneous temperature at the ends of the roller using this approach. An internal, axial flux heater was therefore developed at a seconds stage, and this solution proved to perform better. One advantage with this design that the spacing between the litz wires can be modified at the ends of the roller in order to generate a more uniform heating. A full-scale prototype was then built with this coil design.

The prototype was tested and evaluated in a regular production line for a whole day. In Figure 56 flattening of kebab meat with a heated roll can be seen. The meat is extruded to the left in the figure and moves on the conveyor belt under the induction heated roller towards an oven to the right. The induction heated roller was able to keep the correct temperature and flatten the kebab meat to 2 mm without adhesion problems. The roll measured 1200 mm in width and 200 in diameter, which meant that the moulded SM^2C unit, in the shape of a tube, was one of the largest pieces ever produced with this technology.

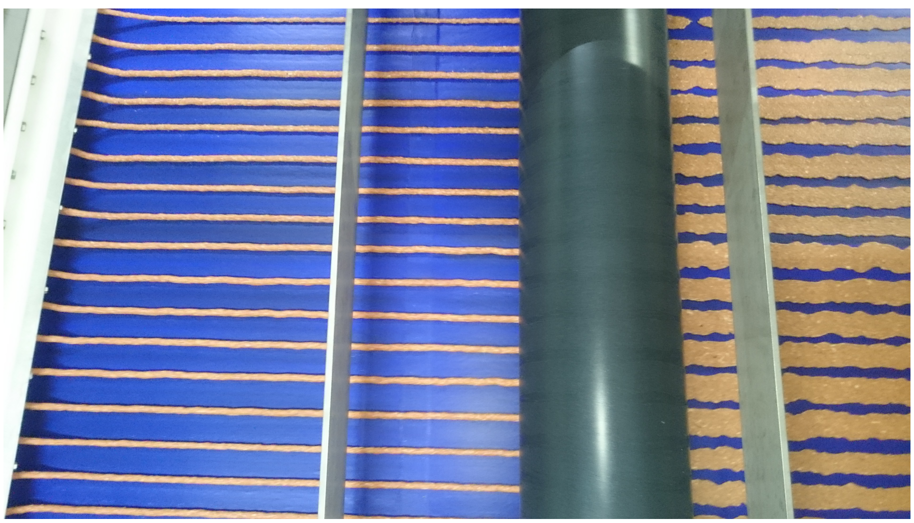

Figure 56: Induction heated roller during production of kebab meat.

8.3 Chokes

Chokes have not been manufactured within the project framework of this thesis, but the general production and material technology has been adopted by a spin-off company, MagComp AB, in their production of chokes. As an example of a typical design and application of a SM^2C choke, one of MagComp's units is presented below.

8.3.1 MagChoke

Traditional chokes are normally produced by either winding a conducting wire around a soft magnetic material or into a pot core. In cases of laminated iron cores, the wire is exposed to the surroundings, which causes magnetic leak fields, energy losses and heating of the surrounding metal. To achieve the targeted inductance, discrete air gaps are required. These air gaps create stray fields and localised hot spots, and so-called air gap losses. Pot cores are visually similar to the MagChoke design, but the coil is not integrated directly into the core, which creates, for instance, hot spots and inefficiencies.

In a MagChoke the electrical coil is placed in the centre of the SM^2C core material, in other words the SM^2C material is moulded around the coil. This design offers maximised thermal coupling between the wire and core material. In this way the MagChoke completely avoids the traditional hot spots in the structure and becomes very homogeneous in thermal performance. The design also minimises the amount of the SM^2C material and the magnetic stray fields, which could disturb other equipment or add losses.

Applications where the MagChoke technology is especially suitable is where inductors must handle a fundamental frequency of, for example, 50 to 300 Hz, while effectively filter higher frequencies generated by switched mode power supplies, for instance. The MagChoke is suitable for both air and liquid-cooled solutions. Examples of suitable products are LC filters, LCL filters and Sinus filters located on the output of frequency inverters.

The application for the choke in Figure 57 is mainly in active harmonic filters. It can be cooled on both sides by aluminium plates that are pressed against the top and bottom surfaces. The choke has a very compact design considering a nominal current of 150 A and 50 μH.

The application for the choke in Figure 58 is a 225 kVA UPS system. It can be cooled on its bottom side by a heat sink. A typical inductance vs current behavior for a MagChoke can be seen in Figure 59.

Figure 57: MagChoke, 50 μH, 150 A, 118 mm diameter, 52 mm height.

Figure 58: MagChoke, 100 μH, 200 A, 180 mm diameter, 76 mm height.

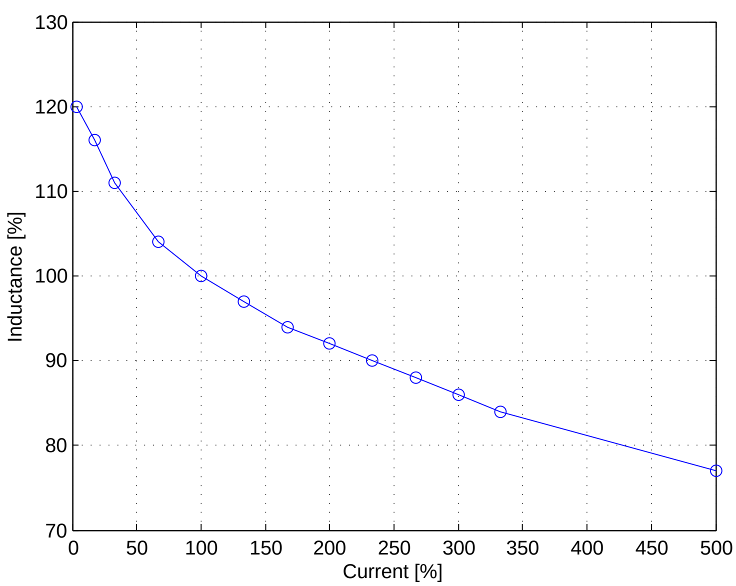

Figure 59: Inductance versus current on a MagChoke. L nominal = 100 % and I nominal = 100 %.

9 Conclusions

A new type of soft magnetic magnetic material has been developed and studied in detail. A main achievement in relation to this work has been to lay the foundation for further development of instrumentation and equipment based on the material. Preparation and measuring methodologies have been developed to suit the respective variants of the material. Data has been gathered and analysed in a manner so that the gained knowledge can be used for customising material properties, such as permeability and thermal conductivity. The developed material has proven to be a useful contribution to the family of soft magnetic composites, especially for the possibility to form complex shapes with practically no limitations in size, while still maintaining necessary functionality.

Some more important conclusions from the thesis are presented below:

- Thermal control and thermal management is essential in order to build more effective induction units and to improve for example efficiency and to reduce size and weight. The study of thermal properties and sources of power losses has therefore been an important task in this work. The calculation of power losses in the system components has been performed through a combination of simulations using material models, and measurement on test samples. The thermal conductivity for both SM^2C materials and various setups of wire bundles and coils have also been carefully measured and studied. The knowledge gained has been used in multiphysics simulations of an induction heater built on SM^2C and litz wire. Through the simulation some important conclusions regarding the interacting materials could be drawn. The parameters which influence the increase in temperature the most in the studied case are the resistivity of the litz wire and the thermal conductivity of the SM^2C material. Here it is more realistic to increase the cross sectional area of the conductor rather than to change the resistivity. The thermal conductivity of the SM^2C could be improved by adding a conductive filler material, without decreasing the particle packing and thereby the permeability. This measure would increase the heat flux and thereby enhance the cooling of the induction heater. A higher output power could thereby be achieved. In general, the study shows that it is essential to get reliable indata for all parameters and properties in the simulation model, as well as establish the connections between different physics systems. A robust model will make it possible to choose from a number of strategies in order to improve materials and performance of the induction unit.

- The technologies used for measuring materials properties in this work are in most cases well established, but design strategies for sample specimen preparation and data evaluation methods have been developed by the author. It is for example important not to mould too small SM^2C samples, because they will generally not reach as high density as larger parts. Smaller test objects should therefore be machined from larger parts, in order to get consistent data on e.g. permeability. A special method for measuring of thermal properties in litz bundles and coils has also been developed. To measure the thermal properties on a non-infiltrated coil a large enough force should be used to hold it together in order to cut and polish the test surface. Specimens with a low copper fill factor will therefore be more difficult to evaluate using this method.

- A number of manufacturing processes for inductors, electrical machines etc. have been developed and evaluated, e.g. rotational casting, vacuum casting and vibrational casting. The vibrational casting or moulding process in combination with a process temperature of 120 °C is found to be the best for most of the material combinations studied. The process temperature in this case could be modified if another matrix material with different viscosity is introduced. A combination of the methods used has not been tested, and could potentially further improve the material. The complexity of combined methods could however be difficult to realize in mass production. The vibrational method has been used on several prototypes and proved to work well.

- Since the SM^2C material and the litz wire are physically very closely connected, due to the moulding process, the electric isolation is of special importance. A thin insulation without air pockets is generally desired, in order to minimize the thermal barrier. However, a short circuit between coil and SM^2C material is fatal, which means that the electric isolation must be given first priority. From the studies performed, it can be concluded that only one layer of coating on the coil is not enough insulation independent on the coating material used. For dip coating, rotating the coil while curing evens out the coating and increases the insulation while at the same time retaining the geometrical properties as well as possible. Powder coating has proven to be the most efficient method to establish a reliable coating for the studied system. In this context it was noted that two layers of powder coating with INFRALIT PE 8350 and six layers of dip coating with

Ultimeg 2000/380 gave roughly the same isolation effect. It can therefore be concluded that the thickness of the individual coating is a more important aspect than the actual coating material chosen.

- The dielectric strength of the SM^2C material is important for long-term use, since a low internal isolation will initiate dielectric breakdown. The performed studies have shown that chokes manufactured from uncoated powder are at risk for this behaviour.
- One important aspect when manufacturing parts from the SM^2C material is to maximize the particle packing in order to maximize the permeability of the material. From the many samples produced, the maximum particle packing reached was 0.72, giving a relative permeability of 25, using uncoated and untreated powder, measured at 10 kHz and 0.1 T. The loss was measured to be 183 kW/m^3 and the dielectric breakdown to be 143 V/m at DC. The reason for the relatively low breakdown voltage is the lack of insulation coating on the particles. A thin insulation layer on each particle without affecting the particle packing would therefore be beneficial.
- There are several benefits introducing the SM^2C material in chokes and in induction heaters; No magnetostriction which means soundless operation; low losses due to the small individually insulated powder particles; no size limitation due to moulding process; simple production due to very few production steps; good thermal coupling between coil and SM^2C structure. The SM^2C material is particularly favourable for large chokes and induction heaters, where the alternative is to assemble multiple small components into one big, costly unit. The same benefits as above applies for electric motors. However, the motors usually require higher permeability and higher saturation than the chokes and induction heaters, in order to obtain a high torque. The SM^2C material could perhaps in some cases be beneficial for high speed and multiple pole motors, which demand high frequency operation.

References

[1] D. Miyagi, A. Saitou, N. Takahashi, N. Uchida, K. Ozaki, Improvement of zone control induction heating equipment for high-speed processing of semiconductor devices, IEEE transactions on magnetics 42 (2) (2006) 292–294.

[2] B. K. Fink, R. L. McCullough, J. W. Gillespie, A local theory of heating in cross-ply carbon fiber thermoplastic composites by magnetic induction, Polymer Engineering & Science 32 (5) (1992) 357–369.

[3] B. K. Fink, R. L. McCullough, J. W. Gillespie, Experimental verification of models for induction heating of continuous-carbon-fiber composites, Polymer composites 17 (2) (1996) 198–209.

[4] J. Davies, Conduction and induction heating, no. 11, IET, 1990.

[5] A. Mühlbauer, History of Induction heating and melting, Vulkan-Verlag GmbH, 2008.

[6] H. Shokouhmand, S. Ghaffari, Thermal analysis of moving induction heating of a hollow cylinder with subsequent spray cooling: Effect of velocity, initial position of coil, and geometry, Applied Mathematical Modelling 36 (9) (2012) 4304–4323.

[7] J. Yun, Y.-S. Yang, Analysis of the induction heating for moving inductor coil, Journal of mechanical science and technology 20 (8) (2006) 1217–1223.

[8] K. Frogner, Industrial induction heating-with a focus on multi coil solutions, Ph.D. thesis, Lund University (2014).

[9] A. Reinap, L. Svensson, M. Alaküla, M. Andersson, Design and evaluation of moulded powder-core machine for in-wheel drive application, in: Electrical Machines (ICEM), 2012 XXth International Conference on, IEEE, 2012, pp. 2629–2634.

[10] L. Siesing, F. Lundström, K. Frogner, T. Cedell, M. Andersson, Towards energy efficient heating in industrial processes three steps to achieve maximized efficiency in an induction heating system, Submitted 2016-07-05 to Applied Thermal Engineering.

[11] L. Svensson, M. Andersson, T. Cedell, P. Jeppsson, Electrical isolation of coils in soft magnetic composite applications, in: 4th Swedish Production Symposium, 2011.

[12] J. Kuffel, E. Kuffel, W. S. Zaengl, High voltage engineering fundamentals, Newnes, 2000.

[13] R. Shuttleworth, G. Bailey, The spreading of a liquid over a rough solid, Discussions of the Faraday Society 3 (1948) 16–22.

[14] J. Oliver, C. Huh, S. Mason, Resistance to spreading of liquids by sharp edges, Journal of Colloid and Interface Science 59 (3) (1977) 568–581.

[15] F. Bartell, J. Shepard, The effect of surface roughness on apparent contact angles and on contact angle hysteresis. i. the system paraffin–water–air, The Journal of Physical Chemistry 57 (2) (1953) 211–215.

[16] L. Siesing, A. Reinap, M. Andersson, Thermal properties on high fill factor electrical windings: Infiltrated vs non infiltrated, in: Electrical Machines (ICEM), 2014 International Conference on, IEEE, 2014, pp. 2218–2223.

[17] N. Simpson, P. Mellor, R. Wrobel, Estimation of equivalent thermal parameters of electrical windings, in: Electrical Machines (ICEM), 2012 XXth International Conference on, IEEE, 2012, pp. 1294–1300.

[18] L. Svensson, K. Frogner, P. Jeppsson, T. Cedell, M. Andersson, Soft magnetic moldable composites: Properties and applications, Journal of Magnetism and Magnetic Materials 324 (18) (2012) 2717–2722.

[19] R. M. Bozorth, Ferromagnetism, Ferromagnetism, by Richard M. Bozorth, pp. 992. ISBN 0-7803-1032-2. Wiley-VCH, August 1993. 1.

[20] B. D. Cullity, C. D. Graham, Introduction to magnetic materials, John Wiley & Sons, 2011.

[21] S. Meier, T. Kjellqvist, S. Norrga, H.-P. Nee, Design considerations for medium-frequency power transformers in offshore wind farms, in: Power Electronics and Applications, 2009. EPE'09. 13th European Conference on, IEEE, 2009, pp. 1–12.

[22] B. W. Williams, Principles and elements of power electronics, BW Williams, 2006.

[23] X. Bi, W. Lan, S. Ou, S. Gong, H. Xu, Magnetic and electrical properties of fesi/fesi–zro 2 multilayers prepared by eb-pvd, Journal of magnetism and magnetic materials 261 (1) (2003) 166–171.

[24] P.-K. Lee, K.-C. Kuo, C.-J. Wu, Z.-T. Wong, J.-Y. Yen, Prediction of iron losses using the modified steinmetz equation under the sinusoidal waveform, in: Control Conference (ASCC), 2011 8th Asian, IEEE, 2011, pp. 579–584.

[25] W. F. Gale, T. C. Totemeier, Smithells metals reference book, Butterworth-Heinemann, 2003.

[26] H. Gavrila, V. Ionita, Crystalline and amorphous soft magnetic materials and their applications- status of art and challenges, Journal of Optoelectronics and Advanced Materials(Romania) 4 (2) (2002) 173–192.

[27] R. Nowosielski, R. Babilas, S. Griner, Z. Stokłosa, Structure and soft magnetic properties of fe72b20si4nb4 bulk metallic glasses, Archives of Materials Science and Engineering 35 (1) (2009) 13–20.

[28] R. U. Lenke, S. Rohde, F. Mura, R. W. De Doncker, Characterization of amorphous iron distribution transformer core for use in high-power medium-frequency applications, in: Energy Conversion Congress and Exposition, 2009. ECCE 2009. IEEE, IEEE, 2009, pp. 1060–1066.

[29] S. Mahmud, A. A. Hossain, A. A. Hakim, M. Seki, T. Kawai, H. Tabata, Influence of microstructure on the complex permeability of spinel type ni–zn ferrite, Journal of Magnetism and Magnetic Materials 305 (1) (2006) 269–274.

[30] H. Shokrollahi, K. Janghorban, Soft magnetic composite materials (smcs), Journal of Materials Processing Technology 189 (1) (2007) 1–12.

[31] Z. W. Lin, J. Zhu, Three-dimensional magnetic properties of soft magnetic composite materials, Journal of magnetism and magnetic materials 312 (1) (2007) 158–163.

[32] L. Siesing, K. Frogner, T. Cedell, M. Andersson, Investigation of thermal losses in a soft magnetic composite using multiphysics modelling and coupled material properties in an induction heating cell, Journal of Electromagnetic Analysis and Applications 8 (9) (2016) 182–196.

[33] ISO 22007-2:2008, Determination of thermal condcutivity and thermal diffusivity–Part2: Transient plane heat source(hot disc) method.

[34] K. Frogner, M. Andersson, T. Cedell, L. Svensson, P. Jeppsson, J.-E. Ståhl, Industrial heating using energy efficient induction technology, in: 44th CIRP Conference on Manufacturing Systems, 2011.

[35] K. Frogner, L. Svensson, M. Andersson, T. Cedell, J.-E. Ståhl, A new concept of coil design for industrial induction heating, in: SPS11, 4th Swedish Production Symposium 2011, 2011.

[36] T. Cedell, P. Jeppsson, M. Andersson, J.-E. Ståhl, C. Högmark, A. Reinap, M. Alaküla, New advances in soft magnetic materials-properties of moulded flux conductors in inductors and electrical motors, in: Inductica Technical Conference, 2009.

[37] K. Frogner, M. Andersson, T. Cedell, L. Svensson, P. Jeppsson, J.-E. Ståhl, Industrial heating using energy efficient induction technology, in: 44th CIRP Conference on Manufacturing Systems, 2011.

[38] K. Frogner, T. Cedell, M. Andersson, Induction heating using a 2-phase travelling wave setup, International Journal of Applied Electromagnetics and Mechanics 44 (2) (2014) 217–226.

[39] A. Reinap, D. Hagstedt, C. Högmark, M. Alaküla, Evaluation of a semi claw-pole machine with sm2c core, in: International Electric Machines and Drives, 2011, pp. 248–253.

[40] A. Reinap, C. Högmark, M. Alaküla, T. Cedell, M. Andersson, An integrated design of sm2c core motor for vehicular applications, in: Electrical Machines (ICEM), 2010 XIX International Conference on, IEEE, 2010.

[41] A. Reinap, M. Alaküla, T. Cedell, M. Andersson, P. Jeppsson, Evaluation of soft magnetic mouldable composite core motors, in: Electrical Machines, 2008. ICEM 2008. 18th International Conference on, IEEE, 2008.

[42] A. Reinap, C. Högmark, M. Alaküla, T. Cedell, M. Andersson, P. Jeppsson, Design and prototyping a torus machine with a rotocast core., in: Electrical Machines, 2008. ICEM 2008. 18th International Conference on, IEEE, 2008.

[43] A. Reinap, M. Alaküla, G. Lindstedt, B. Thuresson, T. Cedell, M. Andersson, P. Jeppsson, An integrated design of a machine with soft magnetic mouldable composite, in: Electrical Machines, 2008. ICEM 2008. 18th International Conference on, IEEE, 2008.

[44] A. Reinap, C. Högmark, M. Alaküla, T. Cedell, M. Andersson, Prototype based study of different winding configurations with sm 2 c core, in: Electrical Machines (ICEM), 2010 XIX International Conference on, IEEE, 2010.

[45] A. Reinap, M. Alaküla, Impact of soft magnetic material on construction of radial flux electrical machines, Magnetics, IEEE Transactions on 48 (4) (2012) 1613–1616.

[46] L. Svensson, A. Reinap, M. Andersson, M. Alaküla, New manufacturing methods for electric motors using different soft magnetic material combinations, in: Electric Drives Production Conference (EDPC), 2012 2nd International, IEEE, 2012, pp. 366–372.

[47] W. Ding, L. Jiang, Y. Liao, J. Song, B. Li, G. Wu, Effect of iron particle size and volume fraction on the magnetic properties of fe/silicate glass soft magnetic composites, Journal of Magnetism and Magnetic Materials 378 (2015) 232–238.

[48] T. C. Hales, A proof of the kepler conjecture, Annals of mathematics 162 (3) (2005) 1065–1185.

[49] G. Scott, D. Kilgour, The density of random close packing of spheres, Journal of Physics D: Applied Physics 2 (6) (1969) 863.

[50] P. Jeppsson, M. Andersson, T. Cedell, A. Reinap, Rotocast-a new methos to produce optimally packed smc components, in: Swedish Production Symposium 2008, 2008.

[51] P. Jeppsson, T. Cedell, M. Andersson, M. Alaküla, A. Reinap, Injection moulding of magnetic flux conductors based on soft magnetic composites, in: Swedish Production Symposium 2007, 2007.

[52] B. Weidenfeller, M. Anhalt, W. Riehemann, Variation of magnetic properties of composites filled with soft magnetic fecov particles by particle alignment in a magnetic field, Journal of Magnetism and Magnetic Materials 320 (14) (2008) e362–e365.

[53] A. Reinap, F. J. Marquez-Fernandez, R. Andersson, C. Högmark, M. Alaküla, A. Gőransson, Heat transfer analysis of a traction machine with directly cooled laminated windings, in: Electric Drives Production Conference (EDPC), 2014 4th International, IEEE, 2014.

[54] C. Högmark, R. Andersson, A. Reinap, M. Alaküla, Electrical machines with laminated winding for hybrid vehicle applications, in: Electric Drives Production Conference (EDPC), 2012 2nd International, IEEE, 2012.

[55] L. Svensson, K. Frogner, A. Reinap, C. Högmark, M. Alaküla, M. Andersson, Alternative production process for electric machine windings, in: Electric Drives Production Conference (EDPC), 2012 2nd International, IEEE, 2012, pp. 161–167.

[56] P. Moratalla, Additive manufacturing: a revolutionary manufacturing solution for hardening coils, heat processing, Vulkan–Verlag 3 2016.

[57] A. G. Jack, B. C. Mecrow, P. G. Dickinson, D. Stephenson, J. S. Burdess, N. Fawcett, J. Evans, Permanent-magnet machines with powdered iron cores and prepressed windings, Industry Applications, IEEE Transactions on 36 (4) (2000) 1077–1084.

[58] R. Wrobel, P. H. Mellor, D. Holliday, Thermal modeling of a segmented stator winding design, Industry Applications, IEEE Transactions on 47 (5) (2011) 2023–2030.

[59] M. Galea, C. Gerada, T. Raminosoa, P. Wheeler, A thermal improvement technique for the phase windings of electrical machines, Industry Applications, IEEE Transactions on 48 (1) (2012) 79–87.

[60] L. Idoughi, X. Mininger, F. Bouillault, L. Bernard, E. Hoang, Thermal model with winding homogenization and fit discretization for stator slot, Magnetics, IEEE Transactions on 47 (12) (2011) 4822–4826.

[61] C. P. Steinmetz, On the law of hysteresis, Transactions of the American Institute of Electrical Engineers 1 (IX) (1892) 1–64.

[62] L. Daniel, R. Corcolle, A note on the effective magnetic permeability of polycrystals, Magnetics, IEEE Transactions on 43 (7) (2007) 3153–3158.

[63] J. Muhlethaler, J. W. Kolar, A. Ecklebe, Loss modeling of inductive components employed in power electronic systems, in: Power Electronics and ECCE Asia (ICPE & ECCE), 2011 IEEE 8th International Conference on, IEEE, 2011, pp. 945–952.

[64] D. C. Meeker, An improved continuum skin and proximity effect model for hexagonally packed wires, Journal of Computational and Applied Mathematics 236 (18) (2012) 4635–4644.

[65] M. Roy, M. Sengupta, Electromagnetic investigations and power converter efficiency studies on a laboratory made induction heating prototype, Journal of The Institution of Engineers (India): Series B 94 (3) (2013) 153–160.

[66] Z. Makni, R. Demersseman, A coupled analytical-numerical approach for optimal sizing of power inductors, COMPEL: The International Journal for Computation and Mathematics in Electrical and Electronic Engineering 33 (5) (2014) 1653–1664.

[67] A. Pusz, Z. Trojnacki, The modelling of thermal conductivity measurements using femm application, Archives of Materials Science and Engineering 53 (1) (2012) 53–60.

[68] Mistra innovation, project-inroll (2016-10-04).
URL `http://www.mistrainnovation.se/projekt/inroll.4.1a9db3-f813af4d6dc46264.html`